Received: 30 September 2023 | Revised: 20 February 2024 | Accepted: 30 March 2024

DOI: 10.1002/nbm.5162

RESEARCH ARTICLE

NMR IN BIOMEDICINE WILEY

Diffusion magnetic resonance imaging of cerebrospinal fluid dynamics: Current techniques and future advancements

Adam M. Wright[1,2] | Yu-Chien Wu[1,2,3] | Li Feng[4] | Qiuting Wen[1,2]

[1]Department of Radiology and Imaging Sciences, Indiana University School of Medicine, Indianapolis, Indiana, USA

[2]Weldon School of Biomedical Engineering Department, Purdue University, West Lafayette, Indiana, USA

[3]Stark Neurosciences Research Institute, Indiana University School of Medicine, Indianapolis, Indiana, USA

[4]Center for Advanced Imaging Innovation and Research (CAI2R), New York University Grossman School of Medicine, New York, New York, USA

Correspondence
Qiuting Wen, Department of Radiology and Imaging Sciences, Indiana University School of Medicine, 355 West 16th Street, Suite 4100, Indianapolis, IN 46202, USA.
Email: wenq@iu.edu

Funding information
This work was funded by the following grants: National Institutes of Health RF1AG083762 (PI: Qiuting Wen) and F30AG084336 (PI: Adam Wright).

Abstract

Cerebrospinal fluid (CSF) plays a critical role in metabolic waste clearance from the brain, requiring its circulation throughout various brain pathways, including the ventricular system, subarachnoid spaces, para-arterial spaces, interstitial spaces, and para-venous spaces. The complexity of CSF circulation has posed a challenge in obtaining noninvasive measurements of CSF dynamics. The assessment of CSF dynamics throughout its various circulatory pathways is possible using diffusion magnetic resonance imaging (MRI) with optimized sensitivity to incoherent water movement across the brain. This review presents an overview of both established and emerging diffusion MRI techniques designed to measure CSF dynamics and their potential clinical applications. The discussion offers insights into the optimization of diffusion MRI acquisition parameters to enhance the sensitivity and specificity of diffusion metrics on underlying CSF dynamics. Lastly, we emphasize the importance of cautious interpretations of diffusion-based imaging, especially when differentiating between tissue- and fluid-related changes or elucidating structural versus functional alterations.

KEYWORDS

cerebrospinal fluid, diffusion-weighted imaging, glymphatic system, interstitial fluid, neurofluid, waste clearance

1 | INTRODUCTION

Cerebrospinal fluid (CSF) envelops and protects the brain while circulating through ventricles, subarachnoid spaces, and paravascular areas (Figure 1). It plays a crucial role in maintaining brain homeostasis and clearing metabolic waste products. Previously, disruptions in CSF circulation were thought to be primarily associated with medical conditions such as hydrocephalus, Chiari malformation, and intracranial hypertension, with no strong links to neurodegenerative diseases. However, with recent scientific developments that have improved researchers' abilities to study CSF circulation, there is increasing evidence that altered CSF dynamics may be linked to neurodegeneration. For example, in 2012–2013, Iliff,

Abbreviations: Δ, diffusion time; 3D TSE, three-dimensional turbo-spin echo; ADC, apparent diffusion coefficient; CSF, cerebrospinal fluid; DTI, diffusion tensor imaging; DWI, diffusion-weighted imaging; dynDWI, dynamic diffusion-weighted imaging; EPI, echo planar imaging; FA, fractional anisotropy; iMDDSDE, improved multi-directional diffusion-sensitized driven-equilibrium preparation; ISF, interstitial fluid; IVIM, intravoxel incoherent motion; MAP-MRI, mean apparent propagator magnetic resonance imaging; MD, mean diffusivity; NODDI, neurite orientation dispersion and density imaging; NPH, normal pressure hydrocephalus; PGSE, pulsed-gradient spin-echo; PVS, perivascular/paravascular space; TE, time echo; TR, time repetition; VENC, velocity-encoding.

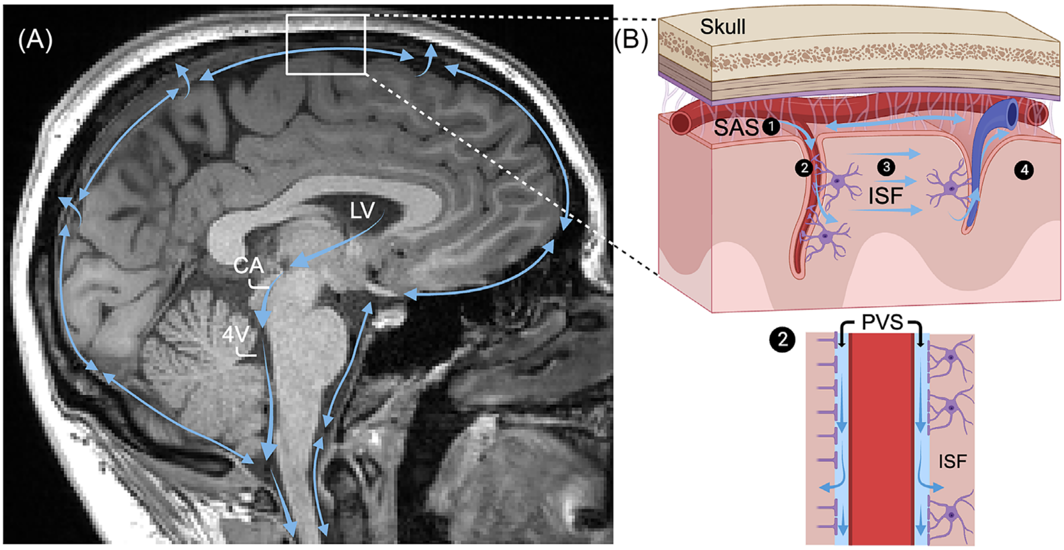

FIGURE 1 Schematic overview of CSF circulation. (A) CSF circulation within the ventricular system and SAS. (B) The microscopic CSF circulation pathway that has been proposed by the glymphatic system hypothesis. CSF circulates from the SAS ① into the para-arterial space ②, then enters the interstitial space ③, and exits through the para-venous space ④. 4V, fourth ventricle; CA, cerebral aqueduct; CSF, cerebrospinal fluid; ISF, interstitial fluid; LV, lateral ventricle; SAS, subarachnoid space; PVS, paravascular space. (Created with BioRender.com).

Nedergaard, and their colleagues published a series of studies that unveiled the crucial role of CSF in eliminating metabolic waste products from the brain through a proposed fluid pathway known as the glymphatic system.[1–4] In this intricate system, CSF flows from the subarachnoid spaces into the brain through para-arterial spaces surrounding cerebral arteries (Figure 1, ① → ②). The CSF actively exchanges with interstitial fluid (ISF) and effectively flushes away waste materials residing between brain cells (Figure 1, ② → ③). Subsequently, the fluid drains waste from the para-venous or perineural spaces (Figure 1, ③ → ④), eventually coursing into the cervical lymph nodes through the meningeal lymphatic vessels and/or nasal lymphatics.[5–9] This pathway is of particular significance because CSF transport can efficiently clear toxic waste proteins that may play a pathological role in neurodegenerative diseases, such as amyloid-beta in Alzheimer's disease. This discovery implies that dysfunction in the fluid dynamics and circulation may be a common disease pathway for various neurodegenerative diseases, making it an attractive target for therapeutic interventions.[7,10,11] Over the past decade, the discovery of the glymphatic system has sparked substantial interest in neuroscience, prompting investigations into its mechanisms, dynamics, and mechanical drivers, and how it changes with normal aging and in neurodegenerative diseases.

The study of glymphatic fluid transport is reliant on in vivo brain imaging because the system's fluid pathways do not withstand tissue fixation.[12] Two-photon imaging has made ground-breaking discoveries of the paravascular CSF pathways, although it is limited to rodent studies and surface-level brain observations. Moreover, it is susceptible to confounds arising from invasive intracranial injections and tracer size dependencies.[13,14] Various magnetic resonance imaging (MRI) techniques have been proposed to study CSF circulation and dynamics, including contrast-enhanced MRI,[15–17] spin-labeling,[18,19] functional MRI,[20–23] and phase-contrast imaging.[24–27] While these techniques have provided valuable insights into CSF flow patterns, they also exhibit limitations. For instance, contrast-enhanced MRI requires the injection of contrast agents, which restricts its frequent use in human studies, spin-labeling can only visualize CSF outflow from specific labeling regions, functional MRI measures are limited to global CSF fluctuations at the fourth ventricle, and phase-contrast imaging solely captures intravoxel coherent flow.

Diffusion MRI offers a noninvasive means of detecting incoherent water movement across the brain and has become one of the most widely used research techniques for studying CSF dynamics. Diffusion MRI employs a pulsed-gradient spin-echo (PGSE) sequence with motion-sensitive gradients, commonly referred to as Stejskal–Tanner diffusion encoding, which provides increased sensitivity to water displacement in the forms of both diffusion and incoherent flow. Traditionally, diffusion MRI has been employed to assess the brain's microstructure by measuring the restricted water diffusivity within neurons and axons, often using a b-value of 1000 s/mm^2 or higher. Considering the physical properties and dynamics of CSF, diffusion MRI is well-suited to image CSF. CSF possesses physical properties similar to water with low protein content and viscosity, resulting in long T2 (~2000 ms)[28] and T1 (~4000 ms)[29] relaxation times at 3 T. Consequently, the T2-weighted contrast in the spin-echo diffusion sequence provides exceptional sensitivity to CSF, with the potential to specifically detect CSF while suppressing signals from blood and tissue by employing a longer echo time (TE). In terms of CSF dynamics, its circulation results from an interplay of different dynamic behaviors, including thermally driven self-diffusion, slow flow associated with circulation, and fluid movement across barriers (e.g., the blood–brain barrier) through filtration and absorption. Diffusion-based imaging can be optimized to be sensitive to all these CSF dynamics. Accordingly, diffusion MRI has been used to investigate most CSF circulation pathways including ventricles, subarachnoid spaces, para-arterial spaces, interstitial spaces, and para-venous spaces. As a result, a wide array of diffusion models and acquisition parameters have been devised to assess these distinct pathways.

This work aims to present a comprehensive review of established and emerging diffusion MRI techniques for assessing fluid dynamics, accompanied by relevant clinical studies. The structure of this review paper is as follows: in Section 2, we describe the distinctive behavior of CSF along various pathways and examine existing theoretical and experimental evidence for using diffusion MRI to quantify these pathways. Section 3 provides an overview of diverse diffusion MRI techniques, organized according to the characteristics of diffusion models. Within this section, we discuss the advantages and limitations associated with each technique. Lastly, we shed light on the opportunities and challenges of applying diffusion MRI to study CSF dynamics.

2 | FLUID DYNAMICS AND THE FEASIBILITY OF DIFFUSION MRI ASSESSMENT

This section reviews the unique fluid dynamics, shown in Figure 2, across various cerebral compartments, including the ventricles, subarachnoid spaces, paravascular space (PVS), and interstitial spaces visualized in Figure 1. It summarizes the applicability of diffusion imaging in measuring these dynamics by drawing from existing theoretical frameworks, experimental investigations, and validation efforts. This section serves as the foundational basis for the subsequent diffusion MRI investigations discussed in Section 3. Note: Given the spatial limitations of diffusion MRI, differentiating between perivascular and paravascular spaces solely based on their anatomical definitions can be challenging.[30–32] Upon reviewing the literature, these terms appear to be used interchangeably by authors, although there may be debates regarding their specific references. In this review, an attempt was made to align with the authors' description by using either perivascular or paravascular terminology as presented in their work.

2.1 | CSF motion in the ventricles and subarachnoid space

In ventricles and subarachnoid space, the CSF dynamics are dependent on the rhythmic movement of the ventricular wall surface,[33,34] the pulsations of cerebral arteries and the brain,[34–39] as well as respiration.[19,40–42] Depending on the location, the slow flow of CSF may be dominated by incoherent flow (Figure 2C, also known as the laminar flow, nonuniform flow, or pseudorandom flow) or coherent flow (Figure 2D), which are both measurable with MRI techniques.

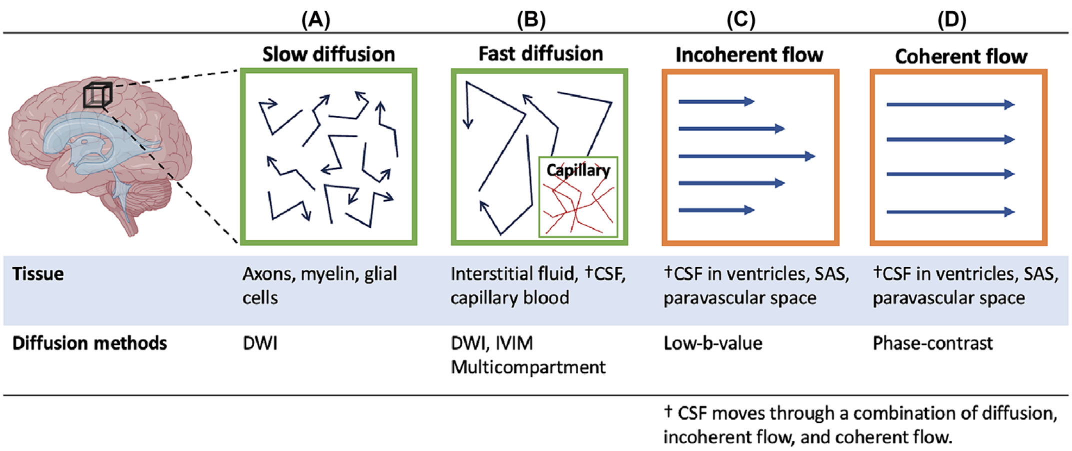

FIGURE 2 Schematic representation of the different types of water movement within a single voxel in relation to their locations in the brain. (A) Slow diffusion, driven by thermally driven random motion, is typically confined to a restricted microstructure environment like axons, myelin, and glial cells. Measurement of the slow diffusion within the tissue microstructure is the primary focus of conventional diffusion MRI techniques. (B) Fast diffusion occurs with less microstructural restriction in areas like interstitial fluid and CSF. Capillary blood, flowing within randomly orientated capillary segments (bottom-right corner), collectively exhibits random motions and may be viewed as pseudodiffusion, often modeled as a fast diffusion compartment in multi-compartment models. (C) Incoherent flow refers to spins within a voxel moving in the same direction at varying velocities; this is also known as laminar or pseudorandom flow. Incoherent flow, such as CSF flow in ventricles and SAS, can be measured using diffusion MRI acquired at lower b-values (b < 500 s/mm^2). (D) Coherent flow occurs when all the spins within a voxel move in the same direction with the same velocity. Faster coherent flow, like CSF in the aqueduct, typically has speeds of approximately 5 cm/s and is usually measured using phase-contrast MRI. Very slow coherent flow in the ventricles and SAS (< 1 cm/s) can be measured using the phase contrast of the diffusion sequence (detailed in Section 3.4). CSF, cerebrospinal fluid; DWI, diffusion-weighted imaging; IVIM, intravoxel incoherent motion; MRI, magnetic resonance imaging; SAS, subarachnoid space. (Created with BioRender.com).

Incoherent flow refers to spins moving within a voxel at varying velocities, either linearly aligned as in laminar flow or randomly oriented as in turbulent flow. The spins accumulate different phases (dephasing) when motion-encoding gradients are applied. This results in a reduction in signal magnitude, detectable through diffusion-weighted imaging (DWI). CSF motion in the ventricles and subarachnoid space is generally characterized as incoherent flow mixed with local stirring induced by the oscillating dynamics due to physiological pulsations. Diffusion MRI has demonstrated its ability to capture the extent of incoherent flow and stirring, although it does not directly measure flow velocity. For example, Bito et al. conducted a mathematical framework illustrating how diffusion imaging at a low b-value (e.g., b < 250 s/mm^2) can detect this incoherent flow.[43] Their calculations showed that the apparent diffusion coefficient (ADC) measures the variance in flow velocity distribution or the intensity of local fluid stirring, which is further dependent on diffusion times.[44] Their human results using b = 100 s/mm^2 reveal elevated ADC in regions known for irregular CSF flow, such as the interventricular foramen, basal cisterns, and lateral sulci. Similarly, simulations by Jang et al. established a robust correlation between diffusivity and CSF flow velocity, affirming a positive relationship between measured diffusivity and flow velocity in the presence of incoherent laminar flow.[45] Further support for diffusion imaging's utility in assessing CSF incoherent flow arises from studies on normal pressure hydrocephalus (NPH) patients, consistently showing reduced diffusivity associated with disrupted or stagnated CSF circulation.[19,46,47] Notably, Le Bihan et al. identified and discussed the potential of low b-value diffusion imaging for detecting nonuniform CSF flow as early as 1986, observing that the ADC value measured in CSF significantly exceeds the diffusion coefficient of free water (2.5 x 10^{-3} mm^2/s at 40°).[48]

By contrast, coherent flow refers to moving spins within a voxel at the same velocity along a consistent direction. For coherently moving spins, motion-encoding gradients introduce a phase shift proportional to the flow velocity, without altering the signal magnitude. This phenomenon can be captured using a gradient-echo or spin-echo sequence with motion-encoding gradients, known as phase-contrast MRI. Phase-contrast MRI has been widely used to measure the coherent CSF flow at the level of the cerebral aqueduct and spinal canal.[36,49,50]

2.2 | Paravascular fluid and interstitial fluid motion within the parenchyma

From the subarachnoid space, CSF flows into the parenchyma through the PVS. It is then further transported into the interstitial space through the AQP4 water channel, forming the ISF, which aids in the removal of waste products located between cells. As a result, paravascular fluid and ISF are the two essential fluid components within the brain parenchyma that hold significant relevance for waste clearance. The PVS is a fluid-filled area surrounding the cerebrovasculature that is visible on heavily T2-weighted images.[51] In contrast to the constrained water diffusion within axons and neurons, paravascular fluid can move more freely parallel to the blood vessels. This motion is commonly modeled as fast diffusion in multi-compartment diffusion approaches (as reviewed in Section 3.3). Beyond diffusion, paravascular space also acts as a conduit for the fluid influx and flows slowly in the same direction as adjacent blood flow.[52,53] In mice, the flow velocity measures around 20 μm/s near major cerebral arteries.[12,54] However, in humans, the velocity of paravascular flow has not yet been directly measured.

The movement of ISF and its exchange with paravascular CSF holds great research interest because of its central role in flushing interstitial waste, as posited by the glymphatic system theory. Over time, debates have arisen concerning whether ISF removes waste products through diffusion or convective flow.[14,55] Recent evidence has begun to converge toward a consensus, indicating a coexistence of both convection and diffusion mechanisms in ISF dynamics.[53,56–58] The extent of their individual contributions is likely contingent upon physiological circumstances.[14] In an effort to explore diffusion imaging's potential to capture the combined convection- and diffusion-driven ISF flow, Komlosh et al. devised an MRI phantom that replicated the tissue environment with added flow. Their experiments with this flow phantom demonstrated that the introduction of flow resulted in an increase in the measured diffusion coefficient, with the most significant increments observed in directions parallel to the flow.[59] These findings support the notion that diffusion imaging can detect the combined effects of diffusion and flow, particularly under specific flow conditions, such as a biologically relevant flow rate of 0.44 mL/min with a Péclet number of 3.31, which is indicative of the convection-to-diffusion ratio.[59] The sensitivity of diffusion imaging in assessing combined diffusion and flow was further corroborated by an animal study, wherein rats treated with an AQP4 facilitator exhibited a significant increase in the measured ADC within the brain tissue.[60] This increase was consistent with enhanced ISF water transport. Similarly, diffusion imaging has also been employed to detect tissue diffusion changes induced by AQP4 inhibitors.[61] However, the authors noted that the precise mechanisms driving these diffusion changes have yet to be explored, given the potentially multifaceted effects of AQP4 inhibitors on astrocytes, interstitial flow, and perfusion.

Together, these studies underscore the potential of utilizing diffusion imaging as a valuable tool for investigating CSF physiology in the ventricles, subarachnoid space, and parenchyma. These findings establish the theoretical and experimental basis for the application of diffusion imaging techniques in the study of CSF dynamics in both normal physiology and pathological conditions, as further discussed in the following section.

3 | CURRENT DIFFUSION MRI APPROACHES

This section reviews existing studies on fluid dynamics using diffusion MRI, which are classified according to their modeling approaches. In certain cases, a specific approach is tailored to measure a particular fluid pathway, such as diffusion tensor imaging along the perivascular space

(DTI-ALPS) for assessing the perivenous space within the brain tissue.[48] Conversely, there are instances where a single approach can be utilized to measure multiple pathways, as seen with intravoxel incoherent motion (IVIM), which measures CSF in ventricular, subarachnoid spaces, and PVS. The organization of this section by diffusion techniques streamlines the presentation of their advantages and limitations. Additionally, we have included a reference table outlining the techniques based on the pathways they assess (Table 1) and a table summarizing their acquisition parameters, advantages, and limitations (Table 2).

3.1 | Mono-compartment diffusion model

3.1.1 | Qualitative evaluations using DWI

Taoka et al. reported the utility of diffusion-weighted contrast at a b-value of 500 s/mm^2 for evaluating CSF dynamics within the cranium.[46,62] Their investigation of ventricles demonstrated that DWI at a b-value of 500 s/mm^2 exhibits greater sensitivity to ventricular CSF motions compared with b = 1000 s/mm^2. In individuals with ventricle dilation, the DWI of b = 500 s/mm^2 showed higher signal intensities compared with controls, indicating reduced CSF flow in conjunction with ventricle dilatation.[46] They extended this approach to a cohort with middle cerebral artery occlusion, revealing the influence of arterial pulsation on CSF motion.[62]

In subsequent work by Taoka et al., the authors acquired DWI across multiple b-values and expanded their investigation to encompass broader CSF-filled spaces within the cranium, including ventricles and subarachnoid spaces.[66] Notably, increased CSF motion was observed in basilar cisterns and lateral sulci compared with frontal and parietal subarachnoid spaces and lateral ventricles. Collectively, these studies propose that DWI with a lower b-value (< 1000 s/mm^2) provides insight into the extent of CSF motion, aligning with prior findings by Le Bihan.[48,92]

The limitations of these methods include their limited quantitative nature and reliance on subjective scoring to assess CSF signal intensity. The absence of cardiac gating can introduce DWI signals dependent on the cardiac cycle, potentially complicating results and interpretation.

TABLE 1 Summary of representative diffusion MRI studies examining fluid dynamics, organized by the anatomical location of interest.

Ventricles and subarachnoid space			Parenchyma		
First author	**Year**	**Model**	**First author**	**Year**	**Model**
Taoka	2019, 2021	Low b-value DWI[46,62]	Thomas	2018	CSF-free[63]
Bito	2021, 2023	Low b-value DTI[43,44]	Sepehrband	2019	CSF-free[64]
Han	2023	Low b-value DTI[65]	Debacker	2020	sADC, SIndex[61]
Jang	2022	Low b-value ADC[45]	Komlosh	2019	DTI[59]
Taoka	2021	Multi b-value DWI[66]	Tuura	2021	DTI[67]
Našel	2007	DTI[47]	Alghanimy	2023	DTI[60]
Le Bihan	1987	IVIM[48]	Taoka	2017	DTI-ALPS[68]
Surer	2018	IVIM[69]	Orzsik	2023	DKI[70]
Becker	2018	IVIM[71]	Demiral	2019	IVIM[72]
Yamada	2023	IVIM[73]	Jiaerken	2021	NODDI[74]
Boye	2018	Phase-contrast[75]	Rau	2021	g-NODDI[76]
Dong	2023	Phase-contrast[77]	Wong	2020	Spectral[78]
Jansen	2020	Phase-contrast[79]	van der Thiel	2021, 2022	Spectral[80,81]
			Drenthen	2023	Spectral[82]
Surface paravascular space[a]					
Ran	2024	Dynamic diffusion[83]			
Harrison	2018	Dynamic diffusion[84]			
Hirschler	2019, 2020, 2022	Dynamic diffusion[85–87]			
Wen	2022	Dynamic diffusion[88,89]			

Abbreviations: ADC, apparent diffusion coefficient; CSF, cerebrospinal fluid; DKI, diffusion kurtosis imaging; DTI-ALPS, diffusion tensor imaging along the perivascular space; DWI, diffusion-weighted imaging; DTI, diffusion tensor imaging; IVIM, intravoxel incoherent motion; g-NODDI, generalization of NODDI using a Bayesian approach; MRI, magnetic resonance imaging; NODDI, neurite orientation dispersion and density imaging; sADC, water diffusion coefficient; SIndex, signature index.

[a]Surface paravascular space refers to the CSF surrounding the major cerebral and/or pial arteries, also known as the perivascular subarachnoid space.[32]

TABLE 2 Overview of diffusion MRI studies on CSF with the inclusion of condensed acquisition information, along with technique advantages and disadvantages.

Section	First author, year	Technique	b-values (s/mm^2) and number of directions	k-space readout	Scan time (min:s)
3.1	Taoka, 2018, 2021	Low b-value DWI[46,62]	b = [0, 500, 1000], 3-directions	2D EPI	< 2:00
3.1	Taoka, 2021	DANDYISM[66]	b = [0, 50, 100, 200, 300, 500, 700, 1000], 3-directions	2D EPI	4:00
3.1	Jang, 2022	Low b-value DWI[45]	20 or 11 b-values in [0-1000], 3-directions	2D EPI	66:00
3.1	Han, 2023	Low b-value DTI[65]	b = 130, 30-directions	2D EPI (TE = 133 ms)	2:00
3.1	Bito, 2023	Low b-value DTI with multiple diffusion times[44]	b = [0, 100, 1000], 13-directions, 3 diffusion times	2D EPI	42:00
3.1	Taoka, 2017	DTI-ALPS[68]	b = 1000, 30-directions	2D EPI	NA
3.2	Thomas, 2018	CSF-free diffusion: bi-exponential fitting model[63]	b = [0, 300, 1100], 3-directions	2D EPI	NA
3.2	Sepehrband, 2019	CSF-free diffusion: bi-tensor model[90]	HCP: b = [0, 1000, 2000, 3,000], 30 or 90 directions; ADNI: b = [500, 1000, 2000], 6, 48, 60 directions, respectively	2D EPI	NA
3.2	Surer, 2018Becker, 2018	Cardiac-gated IVIM[69,71]	b = [0, 5, 10, 20, 35, 55, 80, 110, 150, 200, 300, 500, 750, 1000, 1300], 3-directions	2D EPI	NA
3.2	Yamada, 2023	IVIM[73]	b = [0, 50, 100, 250, 500, 1000], 3-directions	2D EPI	4:00
3.2	Demiral, 2019	IVIM[72]	b = [0, 50, 300, 1000], 3-directions, 16 repeats	2D EPI	16:00
3.2	Örzsik, 2023	DKI/DKTI[70]	b = [0, 800, 2600], 9, 32, 64 directions	2D EPI	8:00
3.2	Rau, 2021	g-NODDI[76]	NA	2D EPI	6:22
3.2	Wong, 2020	Spectral[78]	b = [0, 5, 7, 10, 15, 20, 30, 40, 50, 60, 100, 200, 400, 700, 1000], 1-direction	2D EPI	5:13
3.2	van der Thiel, 2021, 2022	Spectral[80,81]	b = [0, 5, 10, 15, 20, 30, 40, 50, 60, 100, 200, 400, 800, 1000], 3-directions	2D EPI	NA
3.3	Harrison, 2018Evans, 2023	Dynamic diffusion imaging[84,91]	b = 100, 6-directionsb = 43, 2-directions	multishot 2D/3D TSE (TE = 142 or 132 ms)	NA 6:40
3.3	Hirschler, 2019, 2020, 2022	Dynamic diffusion imaging[85–87]	b = 5, 6-directions	multishot 3D TSE (TE = 227 or 497 ms)	40:00
3.3	Ran, 2024	Dynamic diffusion imaging with iMDDSDE preparation[83]	b = 100, 3-directions	multi-shot 3D TSE (TE = 678 ms)	5:00
3.3	Wen, 2022, 2023	Dynamic DWI[88,89]	b = 150, 3-directions	2D EPI	5:00
3.4	Boye, 2017	Phase-contrast velocimetry[75]	b = [50, 200], VENC = 2.6 mm/s, 1.2 mm/s, 1-direction	2D EPI	4:08
3.4	Dong, 2023	Phase-contrast velocimetry[77]	b = N/A, VENC = 10-30 mm/s, 3-directions	2D EPI	NA
3.4	Jansen, 2020	Phase-contrast velocimetry[79]	b = [1400, 2000], VENC = 0.24 mm/s, 30-directions	2D EPI	NA

Abbreviations: ADNI, Alzheimer's disease neuroimaging initiative; CSF, cerebrospinal fluid; DANDYISM, diffusion analysis of fluid dynamics with incremental strength of motion proving gradient; DKI, diffusion kurtosis imaging; DKTI, diffusion kurtosis tensor imaging; DTI, diffusion tensor imaging; DTI-ALPS, diffusion tensor imaging along the perivascular space; DWI, diffusion-weighted imaging; EEG, electroencephalography; EPI, echo planar imaging; g-NODDI, generalization of NODDI using a Bayesian approach; HCP, human connectome project; iMDDSDE, improved multi-directional diffusion-sensitized driven-equilibrium preparation; iNPH, idiopathic NPH; IVIM, intravoxel incoherent motion; MRI, magnetic resonance imaging; NA, not available; NODDI, neurite orientation dispersion and density imaging; NPH, normal pressure hydrocephalus; PVS, paravascular space; SAS, subarachnoid space; TE, echo time; TSE, turbo spin echo; VENC, velocity-encoding. (Disclaimer: The table may contain inaccurate information due to the author's unfamiliarity with certain techniques).

TABLE 2 (Continued)

Section	Field strength (T)	Species	Advantages	Disadvantages	Sequence availability	Postprocessing availability
3.1	1.5/3	Human	Clinically feasible measure	Subjective scoring based on radiologist assessment; no gating to the cardiac cycle	Yes	Yes
3.1	3	Human			Yes	Yes
3.1	7	Rat	Demonstration of a positive relationship between measured diffusivity and CSF velocity	Longer scan time; animal scanning protocol	Yes	No
3.1	3	Human	Long TE to suppress blood flow;high in-plane resolution (1 × 1 mm)	No gating to the cardiac cycle	Yes	Yes
3.1	3	Human	Representative measure of the CSF velocity distribution	Longer scan time; no gating to the cardiac cycle	Yes	No
3.1	3	Human	Clinically feasible measure;retrospective analysis is possible on many clinical datasets	Specificity of measure is undetermined; confounding impact from vascular and neuronal health	Yes	Yes
3.2	3	Human	Accounts for free-water diffusion; clinically feasible measure	Assumptions of isotropy and fixed diffusion limit applicability in PVS	Yes	Unknown
3.2	3	Human	Accounts for anisotropic CSF diffusion; clinically feasible measure	Anatomical assumptions may not hold throughout the brain	Yes	Unknown
3.2	3	Human	Resolves directional and cardiac cycle-related CSF dynamics	Fewer cardiac phases (two trigger delays);small sample size	Yes	Yes
3.2	3	Human	Evaluates IVIM on iNPH cohort with known CSF abnormalities	No gating to the cardiac cycle; measurements in SAS could be subject to partial volume effect	Yes	Yes
3.2	3	Human	Evaluates both during sleep and sleep deprivation changes	Maximum b = 1000 limits restricted diffusion measures	Yes	Yes
3.2	3	Human	Evaluates during sleep changes; assess non-Gaussian diffusion	Suboptimal sleep status monitoring without EEG	Yes	Yes
3.2	3	Human			Yes	No
3.2	3	Human	Accounts for an intermediate diffusion component that may be sensitive to PVS and interstitial fluid	Fitting technique may suffer from robustness challenges	Yes	No
3.2	7	Human			Yes	No
3.3	9.4	Rat	Blood suppression by using a long TE	Limited temporal resolution (4–6 cardiac phases) due to multishot acquisition;timings of diffusion preparation and center k-space at different cardiac phases, necessitating special considerations of data-binning strategy	No	Yes
3.3	7	Human	High spatial resolution (0.45 mm isotropic); Blood/tissue suppression by using a long TE		No	No

(Continues)

TABLE 2 (Continued)

Section	Field strength (T)	Species	Advantages	Disadvantages	Sequence availability	Postprocessing availability
3.3	3	Human	High spatial resolution; short scan time; Long TE with iMDDSDE preparation		No	No
3.3	3	Human	High temporal resolution (50 cardiac phases); robust; clinically feasible measure	Blood suppression using b = 150 is velocity dependent	Yes	No
3.4	3	Human	Quantitative measure of CSF flow velocities	Inconsistent VENC and measured velocities among studies	Yes	Yes
3.4	7	Human			No	No
3.4	3	Human			No	No

Abbreviations: ADNI, Alzheimer's disease neuroimaging initiative; CSF, cerebrospinal fluid; DANDYISM, diffusion analysis of fluid dynamics with incremental strength of motion proving gradient; DKI, diffusion kurtosis imaging; DKTI, diffusion kurtosis tensor imaging; DTI, diffusion tensor imaging; DTI-ALPS, diffusion tensor imaging along the perivascular space; DWI, diffusion-weighted imaging; EEG, electroencephalography; EPI, echo planar imaging; g-NODDI, generalization of NODDI using a Bayesian approach; HCP, human connectome project; iMDDSDE, improved multi-directional diffusion-sensitized driven-equilibrium preparation; iNPH, idiopathic NPH; IVIM, intravoxel incoherent motion; MRI, magnetic resonance imaging; NA, not available; NODDI, neurite orientation dispersion and density imaging; NPH, normal pressure hydrocephalus; PVS, paravascular space; SAS, subarachnoid space; TE, echo time; TSE, turbo spin echo; VENC, velocity-encoding. (Disclaimer: The table may contain inaccurate information due to the author's unfamiliarity with certain techniques).

3.1.2 | Diffusion tensor imaging along the perivascular space

Taoka et al. have developed DTI-ALPS to assess perivascular diffusivity of the medullary veins within the white matter.[68] This technique utilizes a conventional DTI scan with a b-value = 1000 s/mm^2 to quantify water diffusivity along three primary axes. The method cleverly takes advantage of the specific anatomical location lateral to the ventricles, where the medullary veins run perpendicular to a large white matter tract. Because of this anatomical layout, the observed increase in diffusivity parallel to the medullary veins relative to the diffusivity orthogonal to the medullary veins (not aligned with the major white matter tract) is representative of CSF efflux in the PVS of the medullary veins. They named this measurement the ALPS index, which serves as a potential measure of perivenous CSF efflux. The initial study included an Alzheimer's disease cohort, where the authors observed that a decrease in the ALPS index was correlated with worse cognitive function and an increase in age.[68]

Because of the simplicity of the measurement and the ability to retrospectively calculate the ALPS index in large clinical datasets, it has been quickly adopted to study many cerebral health conditions, including neurodegeneration,[68,93–110] cerebrovascular pathologies,[111–117] hydrocephalus,[118–121] epilepsy,[122–128] migraines,[129,130] sleep disorders,[131–134] and traumatic brain injury.[135–137] These studies consistently report a decline in the ALPS index associated with pathology, as well as with an increase in age.[65,138–142]

Although the ALPS index has been quickly adopted and studied in many conditions, the specificity of the ALPS index to perivascular diffusivity remains in question. Because of DTI sensitivity to free-water diffusion and tissue microstructure, it remains unclear how alterations to vascular and neuronal health, independent of the perivascular system, may be impacting the ALPS index.[143] A recent study has provided evidence of white matter contributions to the DTI-ALPS index, suggesting that the decrease in DTI-ALPS in aging and neurodegeneration may be partially attributed to changes in white matter radial asymmetry.[144] Additionally, alterations to the head position and imaging plane have been found to significantly impair the ALPS indices reproducibility,[145] highlighting a need for future studies to control these imaging parameters. Lastly, it remains unclear if the ALPS index has a hemispherical dependence because studies have reported disagreements in statistical significance when comparing the left and right hemispheres.[93,112,136]

3.1.3 | Diffusion tensor imaging with low b-value

Han and colleagues employed low-b DTI (130 s/mm^2 at 30 directions) with a long TE (133 ms) to provide better specificity to CSF dynamics surrounding the middle cerebral arteries.[65] This methodology was applied to a cohort of healthy individuals aged 21–75 years at five different time points throughout 1 day to explore the circadian rhythm dependence of CSF motion. The findings revealed evident anisotropic properties in CSF motion, but the axial diffusivity (along the long axis of the diffusion tensor) exhibited no discernible dependence on the time of day. The lack of cardiac cycle information precluded the assessment of cardiac cycle-dependent CSF motion and its association with time-of-day changes remains unclear.

To gain a deeper understanding of the pseudorandom CSF motion, Bito et al. employed a mathematical approach that modeled the intravoxel pseudorandom CSF motion as a combination of ordered motion (linear/laminar flow, Figure 2C) and disordered motion (diffusion, Figure 2B).[44] They applied low-b DTI (100 s/mm^2 in 13 directions) with three diffusion times to fit the model V_v D_r V_v D_r. V_v D_r and demonstrated the feasibility of investigating the complex CSF dynamics through a novel mathematical framework. This model requires acquisition at multiple diffusion times, leading to longer acquisition times, thereby limiting its feasibility in studying cardiac cycle-dependent CSF dynamics.

3.2 | Multi-compartment diffusion model

3.2.1 | CSF-free diffusion

The CSF-free diffusion model was initially introduced to enhance the accuracy of tissue diffusion measurements by mitigating the partial volume effect caused by CSF.[146,147] This model has been employed to estimate CSF diffusivity and investigate its alterations under physiological conditions,[63] as well as in the context of aging and dementia.[64]

The CSF-free diffusion concept necessitates a multi-b-value DWI acquisition.[147] It employs a biexponential fitting approach to describe the diffusion signal decay across various b-values, assuming two compartments: (i) a parenchymal water pool with a diffusivity lower than that of free water (Figure 2A), characterized by a full tensor; and (ii) an isotropic diffusion water pool with a diffusivity akin to free water at 37°C (Figure 2B). This dual-compartment model serves to decipher the physiological origins of water diffusion alterations, distinguishing between the CSF and tissue water pools.

In the study by Thomas et al., the biexponential fitting model was utilized to explore the impact of time-of-day on brain tissue diffusivity.[63] Similar to the original model, they considered the rapidly diffusing water pool as isotropic with a fixed diffusivity, essentially simulating free water. Their observations revealed an increase in diffusivity from morning to afternoon, primarily in the subarachnoid spaces around cerebral fissures and sulci. This increase was primarily ascribed to the higher volume fraction of free water. They concluded that this variation is due to potential physiological changes of diurnal fluctuations in structural properties of the brain, possibly linked to the glymphatic system. However, a limitation arose from the assumption of isotropy and fixed diffusivity in the rapid-diffusion compartment, which does not accurately model the fluid in the PVS within the parenchyma.

Sepehrband et al. made advancements by proposing a bi-tensor model.[64] This novel approach accommodates anisotropic CSF diffusion without predetermined diffusion values. This adaptability allows the rapid-diffusion compartment to encompass various nonparenchymal fluids, including both "free water" as found in the subarachnoid space and "moderately free water" in the PVS and ISF. To ensure robust fitting, the orientation of the nonparenchymal fluid tensor is constrained to align with the tissue tensor's axis, while maintaining a diffusivity higher than that of the tissue. Their study, which focused on older brains with and without cognitive impairment, revealed that the nonparenchymal fluid component increases with age and neurodegeneration. This aligns with the enlarged PVS and larger water pool seen in aging brains.[51,148] Notably, they emphasized that overlooking nonparenchymal fluid may systematically bias DTI findings. Commonly observed increases in mean diffusivity (MD) and decreases in fractional anisotropy (FA) in neurodegeneration may, in fact, be attributed to changes in the fluid compartment rather than tissue microstructural changes. Their work highlighted the values of the bi-tensor model in disentangling the distinct influences of parenchymal and nonparenchymal diffusion factors. Moreover, their findings underscore the critical significance of accounting for nonparenchymal fluid contribution in DTI studies.

A potential limitation of the model is the assumption of the same alignment of PVS as the white matter tract, which may not hold for all white matter regions. For instance, this assumption may not apply to the PVS of medullary veins, which runs perpendicular to the white matter, as discussed in the DTI-ALPS model.[68] Additionally, the nonparenchymal compartment can be influenced by fluid from multiple sources, including PVS, ISF, and capillary blood, potentially introducing complexity in its interpretation within clinical cohorts. Despite these considerations, this enhanced water-elimination model represents a significant advancement in modeling CSF compartments within brain tissue using a multiple-shell diffusion protocol available in various public databases. The model is particularly valuable for investigating neurodegenerative diseases and distinguishing diffusion changes stemming from alterations in fluid compartments from those related to tissue microstructural changes, which was demonstrated by Sepehrband et al.[90]

3.2.2 | Intravoxel incoherent motion (IVIM) in ventricles and subarachnoid space

IVIM, introduced by Le Bihan et al. in 1987, was designed to distinguish between two tissue compartments within perfused brain tissue[149–151]: (i) the fast-diffusion compartment attributed to the flow of water molecules in randomly oriented capillary segments (Figure 2B, capillary); and (ii) the slow-diffusion compartment resulting from the thermally driven water diffusion (Figure 2A). Remarkably, Le Bihan et al. had also explored the potential of IVIM for measuring ventricular CSF flow in their earlier work in 1986–1987, demonstrating IVIM's sensitivity to slow CSF flows (~1 mm/s) characterized by incoherent motion (laminar or turbulent) within ventricular spaces (Figure 2D).[48,149]

With the renewed interest in fluid dynamics, recent studies have applied cardiac-gated IVIM to investigate the direction and cardiac cycle dependence of CSF movements in the ventricles of healthy brains.[69,71] While Becker et al. focused on lateral ventricles, Surer et al. extended its examination to broader regions encompassing the spinal canal, fourth ventricle, and basal cistern. Both studies unveiled direction-dependent and cardiac cycle-dependent IVIM behaviors within the ventricles. Directionally, a higher fraction of fast diffusion (f) and pseudodiffusion coefficient (D^*) were observed along the high-flow direction, exhibiting spatial variability. For instance, in the lateral ventricles, higher f was noted in the anterior–posterior direction, while in the spinal canal and fourth ventricles, it was evident in the craniocaudal direction.[69,71] These observations align with the expected direction of CSF flow.

Across the cardiac cycle, a significantly higher f was found in systole compared with diastole,[69] or exhibited a trend towards being higher,[71] consistent with previous studies.[152] Notably, neither study observed cardiac cycle dependence or direction dependence in the diffusion coefficient (D). Becker et al. additionally combined phase-contrast MRI to correlate with flow velocity, establishing a moderate to high positive correlation between f and CSF flow. This reinforced the sensitivity of IVIM metrics to CSF flow dynamics and their potential to quantify CSF flow and pulsatility in neurological disorders.Yamada et al. expanded the application of the IVIM model beyond the ventricles to include the subarachnoid space, aiming to investigate patients with NPH,[73] a condition characterized by disrupted CSF circulation. Unlike the previous two studies, they did not utilize cardiac gating in their approach. They consistently found a reduction in f in patients within the ventricles, indicating diminished CSF flow. This reduction was attributed to weakened ciliary movement and reduced brain pulsation.[33,34,39] Within the subarachnoid spaces, reduced f was identified across central and marginal sulci in the NPH group compared with controls. The authors suggested that this decline reflects stagnant CSF flow due to simultaneous ventricle and lateral sulci expansion toward the cranial apex, potentially indicative of glymphatic dysfunction affecting downstream paravascular flow.[39,153–156]

In summary, these investigations collectively suggest that IVIM metrics, notably f, offer valuable insights for assessing complex CSF motion in ventricles and subarachnoid spaces. While the pseudodiffusion coefficient, D^*, theoretically provides the most direct assessment of flow velocity, it exhibits less robustness during the bi-exponential model fitting.[157] Generally, the fraction of fast diffusion f and the slow-diffusion coefficient D

display good stability.[158–161] However, it is important to emphasize that when analyzing the subarachnoid space, cautious interpretation of f is crucial due to the potential partial volume effects with neighboring parenchymal tissue (e.g., gray matter). This is especially relevant at typical imaging resolutions of ≥ $2 \times 2 \times 2\,mm^3$. In the presence of partial volume effects, the observed changes in f may be primarily driven by the extent of partial volume itself. For example, an increase in f observed with aging in the subarachnoid space could be attributed to an expanded CSF fraction resulting from brain atrophy, rather than indicating an actual alteration in CSF flow.

3.2.3 | IVIM within the parenchyma

Within the parenchyma, IVIM reverts to its classical model, where fast diffusion reflects tissue perfusion. Compared with conventional DTI, the slow-diffusion coefficient offers a more precise measure of tissue diffusion. In a study, IVIM was applied to investigate sleep-related differences and the impact of sleep disturbance on IVIM metrics.[72] Building on the animal study findings that sleep increases ISF volume by 40%, the authors hypothesized a corresponding increase in tissue diffusivity.[4] Despite finding an increase in whole-brain CSF volume during sleep based on structural imaging, no alterations in global IVIM metrics were identified. However, the slow diffusion coefficient emerged to be more sensitive in capturing sleep-related changes compared with the rest IVIM metrics, revealing both regional increases and decreases. Concerning sleep disturbances, no differences in IVIM metrics were observed between sleep-deprived wakefulness and rested wakefulness, suggesting that one night of sleep deprivation might not impact tissue diffusion. These findings may hint at a more intricate sleep-related glymphatic function in the human brain compared with rodents. The authors recognized that their maximum b-value of 1000 s/mm^2 could potentially limit the exploration of restricted diffusion in the non-Gaussian ISF or PVS within the parenchyma. They proposed that increasing the b-value to more than 2000 s/mm^2 could amplify sensitivity to non-Gaussian diffusion changes associated with sleep-related alterations.

In line with this, a recent sleep study used high b-value (max. = 2600 s/mm^2) diffusion imaging to assess non-Gaussian changes in ISF during sleep.[70] Using the diffusion kurtosis model, the study revealed a global reduction in both mean and radial kurtosis during sleep. This reduction indicates that water diffusion becomes more Gaussian during sleep, in line with an anticipated increase in interstitial volume fraction. To investigate the origin of reduced diffusion kurtosis—whether it is driven by changes within the interstitial domain or increased fluid exchange across compartments (CSF-ISF exchange)—the researchers conducted a post-hoc analysis using mean apparent propagator MRI (MAP-MRI) analysis.[162,163] Their findings suggest that the observed kurtosis reduction likely originates from increased interstitial volume during sleep, rather than enhanced exchange, aligning with rodent findings.[4] Moreover, their spatial analysis identified regional changes centered on the default mode network, a region most metabolically active when awake and exhibiting slow wave generation during sleep onset, further supporting the model's sensitivity to sleep onset.

In summary, these two studies suggest that diffusion imaging holds the potential for detecting sleep-related ISF changes within the parenchyma, with higher b-values potentially providing better sensitivity to non-Gaussian diffusion changes (kurtosis effect) associated with increased ISF volume during sleep. MAP-MRI could be a useful tool to discern signal origins within intracellular/extracellular domains or across compartment exchanges.

3.2.4 | Neurite orientation dispersion and density imaging (NODDI) in the parenchyma

NODDI, introduced by Zhang et al. in 2012, is a practical diffusion model to assess axonal density and dendrite fanning.[164] NODDI delineates water diffusion into three compartments: (i) free-water diffusion in a water pool; (ii) restricted diffusion within axons and dendrites; and (iii) hindered diffusion in the extracellular space. For free-water diffusion, NODDI employs an isotropic Gaussian diffusion model akin to the aforementioned CSF-free diffusion, with a fixed diffusivity of 3.0×10^{-3} mm^2/s.

While NODDI has primarily been used to assess alterations in axonal density in neurological and neurodegenerative diseases,[165–168] it has more recently been applied to investigate changes in the free-water content of the human brain.[74,76] Jiaerken et al. employed NODDI to examine the free-water content within and around dilated PVS in normal elderly individuals and elderly individuals with cerebral small vessel disease. Their findings revealed consistently elevated free-water content in dilated PVS regions across both groups. However, the surrounding regions near dilated PVS displayed divergent trends, with healthy elderly individuals showing a more pronounced reduction in free-water content.[74] This contrast implies that the dilated PVS may play a distinct role in healthy subjects versus those with cerebral small vessel disease. In another study, Rau et al. utilized NODDI to explore periventricular hyperintensities stemming from transependymal CSF leakage in patients with idiopathic NPH (iNPH). They discovered heightened free-water content in patients compared with controls.[76]

These studies illustrate NODDI's ability to detect free-water content associated with enlarged PVS and ISF within the parenchyma. NODDI shares a similar limitation with the CSF-free model by assuming an isotropic and fixed diffusivity for the free-water compartment. This assumption may not accurately represent the diffusion within the narrow tubular shape of the PVS or the somewhat restricted ISF, potentially limiting NODDI's sensitivity and specificity in studying these fluid components.

3.2.5 | Spectral diffusion analysis in the parenchyma

In the brain parenchyma, both the IVIM and CSF-free diffusion models assume two water compartments. However, the signal within the fast-diffusion compartment may originate from various sources with distinct diffusion properties, including microvascular perfusion, interstitial and paravascular fluid. Recent studies have shown the potential for extracting a third, intermediate diffusion component from cerebral multi-b-value images using spectral fitting methods.[78,80–82,139] This intermediate diffusion component, with diffusivity falling between fast microvascular perfusion and slow tissue diffusion, is believed to primarily represent a combination of interstitial and perivascular fluid, as indicated by its increased presence in regions with enlarged PVS,[80] and in brains affected by cerebral small vessel disease.[78] Unlike the two-compartment model, this three-compartment model may offer improved specificity in capturing changes in paravascular fluid movement. Conducting spectral analysis typically requires the acquisition of a substantial number of b-values (∼15 b-values), and the optimal selection of b-value is discussed by Drenthen et al.[82] While fitting two compartments with three unknowns in IVIM can encounter certain robustness challenges (such as for D^*), fitting three pools with five unknowns in the spectral analysis faces similar challenges, which require further investigation.

3.3 | Low b-value dynamic diffusion imaging

While the multi-compartment models provide measurements of the fluid compartments volume fraction and associated diffusion values, these changes primarily reflect alterations in tissue structures and composition rather than fluid dynamics. For instance, an increased free-water fraction with elevated diffusivity could arise from an enlarged PVS, but not necessarily indicate changes in fluid dynamics. The dynamics aspect of perivascular fluid may be more relevant to the fluid clearance function within the glymphatic system.

To explore fluid dynamics in the PVS, advancements in diffusion imaging have been made in both preclinical and human studies. Perivascular CSF flow can be driven by pulsation, respiratory, and low-frequency oscillation.[58] Pulsation, in particular, has been considered a major driver for CSF influx along the peri-arterial space.[12] Consequently, it has been extensively investigated using prospective or retrospective gating methods. Based on the k-space readout approach, these diffusion techniques can be generally classified into either a multishot three-dimensional turbo-spin-echo (3D TSE) readout or a single-shot 2D echo planar imaging (EPI) readout.

In a pioneering noninvasive preclinical rat study conducted by Harrison et al., DWI using 3D TSE with a b-value of 100 s/mm^2 was used to sensitize the signal to the pulsatile CSF dynamics in the peri-arterial space of the middle cerebral arteries.[84] To suppress the nearby arterial blood with a much shorter T2 than CSF, the authors applied a long echo time (TE = 142 ms). Through prospective gating, they discovered that diffusivity in the PVS was approximately 300% greater during systole compared with diastole, with the principal diffusion direction matching the arterial flow direction. Remarkably, the principal diffusion direction observed was found to be in alignment with the direction of arterial blood flow. This work marked the first noninvasive evidence of pulsation-driven fluid movement in the PVS, with the fluid flow direction mirroring that of the blood flow. A recent application of this technique in acute hypertension revealed diminished CSF directionality in the angiotensin-II pharmacological model, showcasing its potential to advance our understanding of perivascular fluid changes in neurology.[91]

Expanding on this approach to humans, Hirschler et al. developed a high-resolution 3D TSE sequence with sparse reconstruction (compressed sensing), implemented on a 7-T MRI scanner.[85–87] This sophisticated technique achieved high isotropic resolution (0.45 × 0.45 × 0.45 mm^3), allowing for the detection of paravascular fluid dynamics, not only near the middle cerebral arteries, but also within the parenchyma.[87] Their method employed a long echo time (TE = 227 or 497 ms) to effectively suppress the signal from adjacent arterial blood. Using this advanced sequence, they unveiled that CSF movement in the PVS of the human brain is influenced by pulsation, not only near major arteries, but also around smaller penetrating arteries.[86] Additionally, their observations indicated that CSF fluctuations in the PVS, especially those surrounding major arteries, closely follow the cardiac cycle rather than respiratory patterns.[85] Its relatively extended acquisition time (∼40 min) poses challenges for its clinical translation. Along this line, Ran et al. introduced a 3D TSE sequence with a modified diffusion preparation strategy.[83] Notably, they integrated an improved multi-directional diffusion-sensitized driven-equilibrium preparation (iMDDSDE) to address first- and second-order movements of CSF, thereby reducing CSF flow-induced phase errors when combining multishot data. Leveraging compressed sensing techniques, they achieved a remarkable 1 mm isotropic resolution with complete brain coverage in just 5 min, sampled at four cardiac phases. Results revealed that CSF surrounding the middle cerebral artery exhibited the highest diffusivity among major cerebral arteries, with a decline observed in older adults compared with their younger counterparts. Employing this technique on a cohort with cerebral major artery stenosis showed lower CSF diffusivity in individuals with acute ischemia stroke.

Overall, the multishot 3D TSE technique offers notable advantages in achieving extra-long echo times for enhanced blood/tissue suppression and improved image resolution while maintaining a favorable signal-to-noise ratio (SNR). However, a key challenge lies in its inherent limitation to attain high temporal resolution. This limitation stems from the multishot design, constraining the ability to sample many phases across a cardiac cycle within a clinically feasible time. Additionally, the use of a series of 180° pulses during extended readouts may result in temporal averaging of rapidly moving CSF spins. This phenomenon leads to the timings of diffusion preparation and center k-space at different phases of the cardiac cycle, necessitating careful consideration of pulse-triggering and data-binning strategies.[83,86]

Recently, the high temporal resolution of pulsatile CSF dynamics has been achieved using a diffusion-weighted sequence with 2D EPI readout.[88] This technique, named dynamic diffusion-weighted imaging (dynDWI), captures the CSF dynamics at 50 cardiac phases, revealing detailed waveform shapes along major CSF pathways across the brain, including the subarachnoid space and ventricles.[88] It offers specificity to CSF dynamics without the need for ultralong echo times or super-resolution techniques and can be completed in less than 6 min. Specifically, the researchers demonstrated the effectiveness of using a b-value of 150 s/mm^2 to suppress signals from fast-flowing blood spins while maintaining sensitivity to the adjacent CSF. Because the signal of interest involves temporal changes across the cardiac cycle, the contribution of brain tissue to the signal is minimal, making the cardiac cycle-resolved waveforms specific to CSF dynamics. Consistent with prior findings, their results emphasized a strong cardiac dependency of CSF dynamics in the subarachnoid space surrounding cerebral arteries. In an aging cohort, the researchers observed an increase in CSF diffusivity with age and noted alterations in waveform shapes in the older brain, likely reflecting less efficient fluid pumping. Additionally, the higher temporal resolution of dynDWI enabled the study of CSF peak timing, providing relevant insights into cerebral artery stiffness.[89] dynDWI holds significant translational value in uncovering changes in both CSF diffusivity and its waveform shapes. However, it is noteworthy that a b-value of 150 s/mm^2 may not entirely suppress blood flow in all vascular networks. The diffusion gradient's suppression effect is velocity dependent and may compromise suppression in slow-flowing blood like penetrating arterioles and capillaries. This aspect requires systematic evaluations.

In summary, low b-value dynamic diffusion imaging has emerged as a promising approach for assessing paravascular fluid dynamics and their driving forces. Despite its clinical potential, interpreting results requires careful consideration. Specifically, the measured ADC does not directly quantify flow velocity. An increase in diffusivity could indicate either increased fluid velocity[45] or simply intense local fluid mixing.[43] Additionally, the derived tensor direction does not specify whether it is toward or away from a particular point. These nuances should be considered when analyzing and interpreting dynamic diffusion imaging outcomes.

3.4 | Phase-contrast velocimetry using the "diffusion" sequence

All the previously mentioned approaches rely on the diffusion-weighted contrast in the signal magnitude, arising from the incoherent motion of water spins, causing a "dephasing" effect and lowered signal magnitude (Figure 2A–C). However, in the case of CSF flow in the ventricles and subarachnoid space, there exist intravoxel coherently moving spins that travel in parallel with roughly the same velocity (Figure 2D). When motion-sensitive gradients are applied, these spins exhibit a coherent phase shift that is proportional to their flow velocity, allowing for velocimetry. This is the underlying principle of phase-contrast MRI. Nevertheless, phase-contrast MRI typically has a velocity-encoding (VENC) range of 30–200 cm/s, and in some cases as low as 1–5 cm/s, which makes it unsuitable for measuring very slow CSF flow in the subarachnoid space or PVS (< 1 cm/s). On the other hand, PGSE enables longer VENC times and provides more flexibility in setting the VENC values. By employing PGSE with velocity encoding, which is essentially the same as the Stejskal–Tanner diffusion preparation, it becomes feasible to achieve VENC values in the range of 1–10 mm/s or even lower. This makes the diffusion sequence suitable for measuring the exceedingly slow CSF flow in both the ventricular and subarachnoid spaces, where velocity is encoded in the phase of the signal.

Attempts have been made using the diffusion gradient preparation and its phase contrast to measure slow CSF flow. Boye et al. conducted a phantom validation study and showed a good agreement between the measured flow velocity and the ground truth values, demonstrating the feasibility of using diffusion phase images to measure very slow flow (< 2 mm/s).[75] Using this method, they examined the CSF flow velocity in the perineural space of optic nerves in cases of normal tension glaucoma. Their findings indicated a significantly lower CSF velocity in the disease group compared with controls, supporting the notion that compromised CSF flow along the optic nerve may contribute to disease mechanisms.

More recently, two studies employed this approach to study CSF flowmetry and its dynamics in the ventricles and subarachnoid spaces of healthy subjects.[77,79] Both studies detected strong cardiac-coupled CSF flow velocity with varying directions throughout the cardiac cycles. While Jansen et al. used a VENC of 0.1–0.5 mm/s and detected CSF velocity at 0.065 mm/s in the ventricles,[79] Dong et al. used VENC values of 10–30 mm/s and measured velocities of $\sim$10 mm/s in the fourth ventricle and $\sim$1 mm/s in the subarachnoid space.[77] Dong et al. further detected slow CSF flow coupled to both cardiac pulsations and respiration and highlighted the dominant influence of cardiac pulsations over respiration.

These methods offer a notable advantage in their ability to provide quantitative flow velocity measurements. It demonstrates the potential of the diffusion imaging sequence for the simultaneous assessment of both diffusion (using signal magnitude) and flowmetry (using signal phase).[79] However, phase-contrast measurements are susceptible to artifacts arising from gradient hardware imperfections, eddy currents (due to rapid switching of motion-encoding gradients), slice and crusher gradient imperfections, etc. These challenges may be more pronounced when detecting slow flow compared with fast flow. Moreover, the appropriate VENC range for the slow flow in the subarachnoid space remains to be established, given the substantial discrepancies in VENC observed in recent studies.[77,79] An inappropriate VENC setting may lead to phase-wrapping and inaccurate velocity measurements. Additionally, the phase-contrast flowmetry approach may be limited in assessing flow in the smaller PVS within the parenchyma, which requires sufficiently high resolution to observe coherent flow within a voxel. For an in-depth discussion of theories and considerations for measuring slow flow using the PGSE phase regime, readers can refer to Williamson et al.[169]

4 | DISCUSSION

The advancements in existing diffusion techniques demonstrate its remarkable versatility in detecting fluid dynamics. By varying b-values, it can modulate its sensitivity to both diffusion and flow. By altering the direction of the encoding gradient, it can explore the directional dependence of fluid movement. Through dynamic diffusion imaging, it can assess fluid dynamics and uncover the underlying driving forces. Consequently, diffusion imaging emerges as a powerful tool capable of evaluating fluid dynamics across various pathways, including ventricles, subarachnoid space, paravascular space, and interstitial space. Moreover, the inclusion of phase information from the same diffusion sequence enables the assessment of very slow flow velocities, further enhancing the utility and adaptability of diffusion techniques.

While diffusion imaging has yielded novel insights into fluid transport, its heightened sensitivity—advantageous in detecting changes—simultaneously poses a challenge in the interpretation of results. A change in diffusion metrics may have contributions from various tissue components, particularly within the parenchyma. Despite advancements in multi-compartment models, the specificity of diffusion metrics remains somewhat inadequate. This necessitates thorough consideration of potentially confounding factors that may underlie the observed changes, to avoid overinterpretation.

The cautious interpretation becomes particularly pertinent when studying disease cohorts, as changes can occur across the spectrum of tissue components, including neurons, axons, glial cells, ISF content, paravascular fluid content, capillary perfusion, and even the extent of the partial volume effect due to cerebral atrophy. While it is tempting to link diffusivity changes directly to PVS and associated glymphatic function, failure to consider other confounders could undermine the credibility of these discoveries in the long term. Therefore, incorporating validation strategies into study designs is advisable. By recognizing the complex diffusion signal origins and embracing comprehensive validation approaches, the interpretation of diffusion imaging findings can become more robust and informative.

Furthermore, it is crucial not to equate changes in diffusivity with altered fluid flow. Changes in diffusivity may reflect changes in structure or water restriction, unrelated to fluid circulation or glymphatic flow. For instance, an enlarged PVS in aging or disease may lead to changes in diffusivity and the volume fraction of the fast-diffusion compartment. However, these changes may not correlate with modifications in fluid influx or efflux within that space or alterations in glymphatic function. Caution is warranted to avoid conflating "morphological change" with "functional change."

Lastly, careful determination of diffusion imaging parameters (e.g., repetition time [TR], TE, diffusion times) is important to investigate the detailed properties of CSF. Longer TE values can better suppress blood signal (tissue blood T2 $\approx$ 150 ms), but excessively long TE (e.g., > 200 ms) may compromise the SNR with an EPI readout. TR is generally set at longer than 2 s to accommodate the longer T1 recovery of CSF (T1 $\approx$ 3 s) and ensure adequate SNR. Multiband techniques enable a shorter TR of less than 2 s to reduce scan time, albeit at the cost of longitudinal magnetization and SNR. When directionality is not a focus and a trace image suffices, incorporating isotropic diffusion weighting can eliminate the need for encoding in three distinct directions, significantly truncating the scan time by one-third.[170] Another parameter requiring scrutiny and control is the diffusion time (Δ). The diffusion time governs the average distance traversed by spins during imaging and influences measured ADC values when displacement is non-Gaussian, as in incoherent flow (Figure 2D). In such cases, the measured ADC monotonically increases with Δ.[43] Caution should be exercised when comparing ADC values acquired at varying diffusion times, even with the same b-value.

In conclusion, diffusion MRI has emerged as a potent tool for noninvasively probing CSF dynamics within the human brain, a previously overlooked signal pool that has now gained paramount importance in the context of brain health. Given the rapidly growing application of diffusion MRI in CSF research, it is imperative to approach result interpretation with caution, especially when confronted with the need to distinguish between tissue- and fluid-related changes or to elucidate structural versus functional alterations. Future research efforts may prioritize the development of diffusion MRI techniques capable of providing enhanced signal specificity to the fluid compartment. This potential avenue holds significant promise for further exploration and advancement in the field.

ACKNOWLEDGMENTS

Figures 1 and 2 were created with BioRender.com. This work was funded by the following grants: National Institutes of Health RF1AG083762 (PI: Qiuting Wen) and F30AG084336 (PI: Adam Wright).

CONFLICT OF INTEREST STATEMENT

The authors have no conflicts of interest to disclose.

ORCID

Adam M. Wright https://orcid.org/0000-0001-9524-2210
Yu-Chien Wu https://orcid.org/0000-0003-1084-2634
Li Feng https://orcid.org/0000-0002-8692-7645
Qiuting Wen https://orcid.org/0000-0002-7885-4036

REFERENCES

1. Iliff JJ, Wang M, Liao Y, et al. A paravascular pathway facilitates CSF flow through the brain parenchyma and the clearance of interstitial solutes, including amyloid β. *Sci Transl Med*. 2012;4(147):147ra111-147ra111. doi:10.1126/scitranslmed.3003748
2. Iliff JJ, Lee H, Yu M, et al. Brain-wide pathway for waste clearance captured by contrast-enhanced MRI. *J Clin Invest*. 2013;123(3):1299-1309. doi:10.1172/JCI67677
3. Iliff JJ, Wang M, Zeppenfeld DM, et al. Cerebral arterial pulsation drives paravascular CSF-Interstitial fluid exchange in the murine brain. *J Neurosci*. 2013;33(46):8190-18199. doi:10.1523/JNEUROSCI.1592-13.2013
4. Xie L, Kang H, Xu Q, et al. Sleep drives metabolite clearance from the adult brain. *Science*. 2013;342(6156):373-377. doi:10.1126/SCIENCE.1241224/SUPPL_FILE/XIE-SM.PDF
5. Yoon JH, Jin H, Kim HJ, et al. Nasopharyngeal lymphatic plexus is a hub for cerebrospinal fluid drainage. *Nature*. 2024;625(7996):768-777. doi:10.1038/s41586-023-06899-4
6. Kida S, Pantazis A, Weller RO. CSF drains directly from the subarachnoid space into nasal lymphatics in the rat. Anatomy, histology and immunological significance. *Neuropathol Appl Neurobiol*. 1993;19(6):480-488. doi:10.1111/j.1365-2990.1993.tb00476.x
7. Wen Q, Wang H, Haacke EM, Jiang Q, Hu J. Contribution of direct cerebral vascular transport in brain substance clearance. *Aging Dis*. 2023. doi:10.14336/AD.2023.0426
8. Louveau A, Smirnov I, Keyes TJ, et al. Structural and functional features of central nervous system lymphatic vessels. *Nature*. 2015;523(7560):337-341. doi:10.1038/nature14432
9. Aspelund A, Antila S, Proulx ST, et al. A dural lymphatic vascular system that drains brain interstitial fluid and macromolecules. *J Exp Med*. 2015;212(7):991-999. doi:10.1084/jem.20142290
10. Nedergaard M, Goldman SA. Glymphatic failure as a final common pathway to dementia. *Science*. 2020;370(6512):50-56. doi:10.1126/science.abb8739
11. Lv T, Zhao B, Hu Q, Zhang X. The glymphatic system: a novel therapeutic target for stroke treatment. *Front Aging Neurosci*. 2021;13:689098. doi:10.3389/fnagi.2021.689098
12. Mestre H, Tithof J, Du T, et al. Flow of cerebrospinal fluid is driven by arterial pulsations and is reduced in hypertension. *Nat Commun*. 2018;9(1):4878. doi:10.1038/s41467-018-07318-3
13. Zhu Y, Wang G, Kolluru C, et al. Transport pathways and kinetics of cerebrospinal fluid tracers in mouse brain observed by dynamic contrast-enhanced MRI. *Sci Rep*. 2023;13(1):13882. doi:10.1038/s41598-023-40896-x
14. Mestre H, Mori Y, Nedergaard M. The brain's glymphatic system: current controversies. *Trends Neurosci*. 2020;43(7):458-466. doi:10.1016/j.tins.2020.04.003
15. Ringstad G, Vatnehol SAS, Eide PK. Glymphatic MRI in idiopathic normal pressure hydrocephalus. *Brain*. 2017;140(10):2691-2705. doi:10.1093/brain/awx191
16. Naganawa S, Nakane T, Kawai H, Taoka T. Lack of contrast enhancement in a giant perivascular space of the basal ganglion on delayed FLAIR images: implications for the glymphatic system. *Magn Reson Med Sci*. 2017;16(2):89-90. doi:10.2463/mrms.ci.2016-0114
17. Cao D, Sun Y, Li Y, et al. Concurrent measurement of perfusion parameters related to small blood vessels and cerebrospinal fluid circulation in the human brain using dynamic dual-spin-echo perfusion MRI. *NMR Biomed*. 2023;36(10):e4984. doi:10.1002/nbm.4984
18. Petitclerc L, Hirschler L, Wells JA, et al. Ultra-long-TE arterial spin labeling reveals rapid and brain-wide blood-to-CSF water transport in humans. *Neuroimage*. 2021;245:118755. doi:10.1016/j.neuroimage.2021.118755
19. Yamada S, Miyazaki M, Kanazawa H, et al. Visualization of cerebrospinal fluid movement with spin labeling at MR imaging: preliminary results in normal and pathophysiologic conditions. *Radiology*. 2008;249(2):644-652. doi:10.1148/radiol.2492071985
20. Kiviniemi V, Wang X, Korhonen V, et al. Ultra-fast magnetic resonance encephalography of physiological brain activity-Glymphatic pulsation mechanisms? *J Cereb Blood Flow Metab*. 2016;36(6):1033-1045. doi:10.1177/0271678X15622047
21. Fultz NE, Bonmassar G, Setsompop K, et al. Coupled electrophysiological, hemodynamic, and cerebrospinal fluid oscillations in human sleep. *Science*. 2019;366(6465):628-631. doi:10.1126/science.aax5440
22. Yang HC, Inglis B, Talavage TM, et al. Coupling between cerebrovascular oscillations and CSF flow fluctuations during wakefulness: an fMRI study. *J Cereb Blood Flow Metab*. 2022;42(6):1091-1103. doi:10.1177/0271678X221074639
23. Vijayakrishnan Nair V, Kish BR, Inglis B, et al. Human CSF movement influenced by vascular low frequency oscillations and respiration. *Front Physiol*. 2022;13:940140. doi:10.3389/fphys.2022.940140
24. Zhu DC, Xenos M, Linninger AA, Penn RD. Dynamics of lateral ventricle and cerebrospinal fluid in normal and hydrocephalic brains. *J Magn Reson Imaging*. 2006;24(4):756-770. doi:10.1002/jmri.20679
25. Battal B, Kocaoglu M, Bulakbasi N, Husmen G, Tuba Sanal H, Tayfun C. Cerebrospinal fluid flow imaging by using phase-contrast MR technique. *Br J Radiol*. 2011;84(1004):758-765. doi:10.1259/bjr/66206791
26. Liu P, Fall S, Balédent O. Use of real-time phase-contrast MRI to quantify the effect of spontaneous breathing on the cerebral arteries. *Neuroimage*. 2022;258:119361. doi:10.1016/j.neuroimage.2022.119361
27. Yatsushiro S, Sunohara S, Hayashi N, et al. Cardiac-driven pulsatile motion of intracranial cerebrospinal fluid visualized based on a correlation mapping technique. *Magn Reson Med Sci*. 2018;17(2):151-160. doi:10.2463/mrms.mp.2017-0014
28. Spijkerman JM, Petersen ET, Hendrikse J, Luijten P, Zwanenburg JJM. T2 mapping of cerebrospinal fluid: 3 T versus 7 T. *MAGMA*. 2018;31(3):415-424. doi:10.1007/s10334-017-0659-3
29. Shin W, Gu H, Yang Y. Fast high-resolution T1 mapping using inversion-recovery look-locker echo-planar imaging at steady state: optimization for accuracy and reliability. *Magn Reson Med*. 2009;61(4):899-906. doi:10.1002/mrm.21836
30. Faghih MM, Sharp MK. Is bulk flow plausible in perivascular, paravascular and paravenous channels? *Fluids Barriers CNS*. 2018;15(1):17. doi:10.1186/s12987-018-0103-8
31. Bakker ENTP, Bacskai BJ, Arbel-Ornath M, et al. Lymphatic Clearance of the Brain: Perivascular, Paravascular and Significance for Neurodegenerative Diseases. *Cell Mol Neurobiol*. 2016;36(2):181-194. doi:10.1007/s10571-015-0273-8
32. Eide PK, Ringstad G. Functional analysis of the human perivascular subarachnoid space. *Nat Commun*. 2024;15(1). doi:10.1038/s41467-024-46329-1

33. Ohata S, Nakatani J, Herranz-Pérez V, et al. Loss of Dishevelleds disrupts planar polarity in ependymal motile cilia and results in hydrocephalus. *Neuron.* 2014;83(3):558-571. doi:10.1016/j.neuron.2014.06.022
34. Olstad EW, Ringers C, Hansen JN, et al. Ciliary beating compartmentalizes cerebrospinal fluid flow in the brain and regulates ventricular development. *Curr Biol.* 2019;29(2):229-241.e6. doi:10.1016/j.cub.2018.11.059
35. Bradley WG. CSF flow in the brain in the context of normal pressure hydrocephalus. *Am J Neuroradiol.* 2015;36(5):831-838. doi:10.3174/AJNR.A4124
36. Laganà MM, Di Tella S, Ferrari F, et al. Blood and cerebrospinal fluid flow oscillations measured with real-time phase-contrast MRI: breathing mode matters. *Fluids Barriers CNS.* 2022;19(1):100. doi:10.1186/s12987-022-00394-0
37. Yamada S, Ishikawa M, Ito H, et al. Cerebrospinal fluid dynamics in idiopathic normal pressure hydrocephalus on four-dimensional flow imaging. *Eur Radiol.* 2020;30(8):4454-4465. doi:10.1007/s00330-020-06825-6
38. Yamada S, Ito H, Ishikawa M, et al. Quantification of oscillatory shear stress from reciprocating CSF motion on 4D flow imaging. *Am J Neuroradiol.* 2021;42(3):479-486. doi:10.3174/AJNR.A6941
39. Yamada S, Ishikawa M, Nozaki K. Exploring mechanisms of ventricular enlargement in idiopathic normal pressure hydrocephalus: a role of cerebrospinal fluid dynamics and motile cilia. *Fluids Barriers CNS.* 2021;18(1):20. doi:10.1186/s12987-021-00243-6
40. Yamada S, Miyazaki M, Yamashita Y, et al. Influence of respiration on cerebrospinal fluid movement using magnetic resonance spin labeling. *Fluids Barriers CNS.* 2013;10(1):36. doi:10.1186/2045-8118-10-36
41. Yamada S, Tsuchiya K, Bradley WG, et al. Current and emerging MR imaging techniques for the diagnosis and management of CSF flow disorders: a review of phase-contrast and time-spatial labeling inversion pulse. *Am J Neuroradiol.* 2015;36(4):623-630. doi:10.3174/ajnr.A4030
42. Yatsushiro S, Sunohara S, Matsumae M, et al. Evaluation of cardiac-and respiratory-driven cerebrospinal fluid motions by applying the S-transform to steady-state free precession phase contrast imaging. *Magn Reson Med Sci.* 2022;21(2):372-379. doi:10.2463/mrms.mp.2021-0126
43. Bito Y, Harada K, Ochi H, Kudo K. Low b-value diffusion tensor imaging for measuring pseudorandom flow of cerebrospinal fluid. *Magn Reson Med.* 2021;86(3):1369-1382. doi:10.1002/mrm.28806
44. Bito Y, Ochi H, Shirase R, Yokohama W, Harada K, Kudo K. Low b-value diffusion tensor imaging to analyze the dynamics of cerebrospinal fluid: resolving intravoxel pseudorandom motion into ordered and disordered motions. *Magn Reson Med Sci*. Published online. October 27, 2023. Epub ahead of print. doi:10.2463/mrms.mp.2023-0081
45. Jang MJ, Han SH, Cho HJ. D* from diffusion MRI reveals a correspondence between ventricular cerebrospinal fluid volume and flow in the ischemic rodent model. *J Cereb Blood Flow Metab.* 2022;42(4):572-583. doi:10.1177/0271678X211060741
46. Taoka T, Naganawa S, Kawai H, Nakane T, Murata K. Can low b value diffusion weighted imaging evaluate the character of cerebrospinal fluid dynamics? *Jpn J Radiol.* 2019;37(2):135-144. doi:10.1007/s11604-018-0790-8
47. Našel C, Gentzsch S, Heimberger K. Diffusion-weighted magnetic resonance imaging of cerebrospinal fluid in patients with and without communicating hydrocephalus. *Acta Radiol.* 2007;48(7):768773. doi:10.1080/02841850701408251
48. Le Bihan D, Breton E, Aubin ML, Lallemand D, Vignaud J. Study of cerebrospinal fluid dynamics by MRI of intravoxel incoherent motions (IVIM). *J Neuroradiol.* 1987;14(4):388-395.
49. Kollmeier JM, Gürbüz-Reiss L, Sahoo P, et al. Deep breathing couples CSF and venous flow dynamics. *Sci Rep.* 2022;12(1):2568. doi:10.1038/s41598-022-06361-x
50. Alperin N, Vikingstad EM, Gomez-Anson B, Levin DN. Hemodynamically independent analysis of cerebrospinal fluid and brain motion observed with dynamic phase contrast MRI. *Magn Reson Med.* 1996;35(5):741-754. doi:10.1002/mrm.1910350516
51. Wardlaw JM, Benveniste H, Nedergaard M, et al. Perivascular spaces in the brain: anatomy, physiology and pathology. *Nat Rev Neurol.* 2020;16(3):137-153. doi:10.1038/s41582-020-0312-z
52. Thomas JH. Fluid dynamics of cerebrospinal fluid flow in perivascular spaces. *J R Soc Interface.* 2019;16(159):20190572. doi:10.1098/rsif.2019.0572
53. Kelley DH, Thomas JH. Cerebrospinal fluid flow. *Annu Rev Fluid Mech*. 2023;55(1):237-264. doi:10.1146/annurev-fluid-120720-011638
54. Bedussi B, Almasian M, de Vos J, VanBavel E, Bakker ENTP. Paravascular spaces at the brain surface: low resistance pathways for cerebrospinal fluid flow. *J Cereb Blood Flow Metab*. 2018;38(4):746. doi:10.1177/0271678X17737984
55. Klostranec JM, Vucevic D, Bhatia KD, et al. Current concepts in intracranial interstitial fluid transport and the glymphatic system: part ii-imaging techniques and clinical applications. *Radiology*. 2021;301(3):516-532. doi:10.1148/radiol.2021204088
56. Valnes LM, Mitusch SK, Ringstad G, Eide PK, Funke SW, Mardal KA. Apparent diffusion coefficient estimates based on 24 hours tracer movement support glymphatic transport in human cerebral cortex. *Sci Rep*. 2020;10(1):9176. doi:10.1038/s41598-020-66042-5
57. Kounda S, Elkin R, Nadeem S, et al. Optimal mass transport with lagrangian workflow reveals advective and diffusion driven solute transport in the glymphatic system. *Sci Rep*. 2020;10(1):1990. doi:10.1038/s41598-020-59045-9
58. Rasmussen MK, Mestre H, Nedergaard M. Fluid transport in the brain. *Physiol Rev*. 2022;102(2):1025-1151. doi:10.1152/physrev.00031.2020
59. Komlosh ME, Benjamini D, Williamson NW, Horkay F, Hutchinson EB, Basser PJ. A novel MRI phantom to study interstitial fluid transport in the glymphatic system. *Magn Reson Imaging*. 2019;56. doi:10.1016/j.mri.2018.10.007
60. Alghanimy A, Martin C, Gallagher L, Holmes WM. The effect of a novel AQP4 facilitator, TGN-073, on glymphatic transport captured by diffusion MRI and DCE-MRI. *PLoS ONE*. 2023;18(3):e0282955. doi:10.1371/journal.pone.0282955
61. Debacker C, Djemai B, Ciobanu L, Tsurugizawa T, Le BD. Diffusion MRI reveals in vivo and non-invasively changes in astrocyte function induced by an aquaporin-4 inhibitor. *PLoS ONE.* 2020;15(5):e0235581. doi:10.1371/journal.pone.0229702
62. Taoka T, Kawai H, Nakane T, et al. Evaluating the effect of arterial pulsation on cerebrospinal fluid motion in the sylvian fissure of patients with middle cerebral artery occlusion using low b-value diffusion-weighted imaging. *Magn Reson Med Sci.* 2021;20(4):371-377. doi:10.2463/mrms.mp.2020-0121
63. Thomas C, Sadeghi N, Nayak A, et al. Impact of time-of-day on diffusivity measures of brain tissue derived from diffusion tensor imaging. *Neuroimage.* 2018;173:25-34. doi:10.1016/j.neuroimage.2018.02.026
64. Sepehrband F, Cabeen RP, Choupan J, Barisano G, Law M, Toga AW. Perivascular space fluid contributes to diffusion tensor imaging changes in white matter. *Neuroimage.* 2019;197:243-254. doi:10.1016/j.neuroimage.2019.04.070
65. Han G, Zhou Y, Zhang K, et al. Age- and time-of-day dependence of glymphatic function in the human brain measured via two diffusion MRI methods. *Front Aging Neurosci.* 2023;15:1173221. doi:10.3389/fnagi.2023.1173221

66. Taoka T, Kawai H, Nakane T, et al. Diffusion analysis of fluid dynamics with incremental strength of motion proving gradient (DANDYISM) to evaluate cerebrospinal fluid dynamics. *Jpn J Radiol.* 2021;39(4):315-323. doi:10.1007/s11604-020-01075-4
67. Tuura ROG, Volk C, Callaghan F, Jaramillo V, Huber R. Sleep-related and diurnal effects on brain diffusivity and cerebrospinal fluid flow. *Neuroimage.* 2021;241:118420. doi:10.1016/j.neuroimage.2021.118420
68. Taoka T, Masutani Y, Kawai H, et al. Evaluation of glymphatic system activity with the diffusion MR technique: diffusion tensor image analysis along the perivascular space (DTI-ALPS) in Alzheimer's disease cases. *Jpn J Radiol.* 2017;35(4):172-178. doi:10.1007/s11604-017-0617-z
69. Surer E, Rossi C, Becker AS, et al. Cardiac-gated intravoxel incoherent motion diffusion-weighted magnetic resonance imaging for the investigation of intracranial cerebrospinal fluid dynamics in the lateral ventricle: a feasibility study. *Neuroradiology.* 2018;60(4):413-419. doi:10.1007/s00234-018-1995-3
70. Örzsik B, Palombo M, Asllani I, Dijk DJ, Harrison NA, Cercignani M. Higher order diffusion imaging as a putative index of human sleep-related microstructural changes and glymphatic clearance. *Neuroimage.* 2023;274:120124. doi:10.1016/j.neuroimage.2023.120124
71. Becker AS, Boss A, Klarhoefer M, Finkenstaedt T, Wurnig MC, Rossi C. Investigation of the pulsatility of cerebrospinal fluid using cardiac-gated Intravoxel Incoherent motion imaging. *Neuroimage.* 2018;169:126-133. doi:10.1016/j.neuroimage.2017.12.017
72. Demiral ŞB, Tomasi D, Sarlls J, et al. Apparent diffusion coefficient changes in human brain during sleep—does it inform on the existence of a glymphatic system? *Neuroimage.* 2019;185:263-273. doi:10.1016/j.neuroimage.2018.10.043
73. Yamada S, Hiratsuka S, Otani T, et al. Usefulness of intravoxel incoherent motion MRI for visualizing slow cerebrospinal fluid motion. *Fluids Barriers CNS.* 2023;20(1):16. doi:10.1186/s12987-023-00415-6
74. Jiaerken Y, Lian C, Huang P, et al. Dilated perivascular space is related to reduced free-water in surrounding white matter among healthy adults and elderlies but not in patients with severe cerebral small vessel disease. *J Cereb Blood Flow Metab.* 2021;41(10):2561-2570. doi:10.1177/0271678X211005875
75. Boye D, Montali M, Miller NR, et al. Flow dynamics of cerebrospinal fluid between the intracranial cavity and the subarachnoid space of the optic nerve measured with a diffusion magnetic resonance imaging sequence in patients with normal tension glaucoma. *Clin Exp Ophthalmol.* 2018;46(5):511-518. doi:10.1111/ceo.13116
76. Rau A, Reisert M, Kellner E, Hosp JA, Urbach H, Demerath T. Increased interstitial fluid in periventricular and deep white matter hyperintensities in patients with suspected idiopathic normal pressure hydrocephalus. *Sci Rep.* 2021;11(1):19552. doi:10.1038/s41598-021-98054-0
77. Dong Z, Wang F, Strom AK, et al. 4D CSF flowmetry to map brain-wide slow CSF flow dynamics and patterns in subarachnoid space. In: *Proc. Intl. Soc. Mag. Reson. Med*; 2023.
78. Wong SM, Backes WH, Drenthen GS, et al. Spectral diffusion analysis of intravoxel incoherent motion MRI in cerebral small vessel disease. *J Magn Reson Imaging.* 2020;51(4):1170-1180. doi:10.1002/jmri.26920
79. Jansen IH, Marinelli L, Tsoon Tan E, et al. Simultaneous Imaging of diffusion and coherent motion in slow-flow compartments in the brain. In: *Proc. Intl. Soc. Mag. Reson. Med.* Luca Marinelli; 2020.
80. van der Thiel M, Roos N, Drenthen G, et al. On the origin of a potential clearance marker: the contribution of enlarged perivascular fluid diffusion to a 7T IVIM interstitial fluid proxy. In: *ISMRM*; 2022:0326. doi:10.58530/2022/0326
81. van der Thiel MM, Freeze WM, Verheggen ICM, et al. Associations of increased interstitial fluid with vascular and neurodegenerative abnormalities in a memory clinic sample. *Neurobiol Aging.* 2021;106:257-267. doi:10.1016/j.neurobiolaging.2021.06.017
82. Drenthen GS, Jansen JFA, van der MM, PHM V, Backes WH. An optimized b-value sampling for the quantification of interstitial fluid using diffusion-weighted MRI, a genetic algorithm approach. *Magn Reson Med.* 2023;90(1):194-201. doi:10.1002/mrm.29612
83. Ran L, He Y, Zhu J, et al. Characterizing cerebrospinal fluid mobility using heavily T2-weighted 3D fast spin echo (FSE) imaging with improved multi-directional diffusion-sensitized driven-equilibrium (iMDDSDE) preparation. *J Cereb Blood Flow Metab.* 2024;44(1):105-117. doi:10.1177/0271678X231194863
84. Harrison IF, Siow B, Akilo AB, et al. Non-invasive imaging of CSF-mediated brain clearance pathways via assessment of perivascular fluid movement with diffusion tensor MRI. *Elife.* 2018;7. doi:10.7554/eLife.34028
85. Hirschler L, Runderkamp B, van Veluw S, Caan M, van Osch M. Effects of the cardiac and respiratory cycles on CSF-mobility in human subarachnoid and perivascular spaces. In: *ISMRM*; 2022:0320. doi:10.58530/2022/0320
86. Hirschler L, Runderkamp BA, Franklin S, et al. The driving force of glymphatics: influence of the cardiac cycle on CSF-mobility in perivascular spaces in humans. *Proc Intl Soc Mag Reson Med.* 2020:28.
87. Hirschler L, Aldea R, Petitclerc L, et al. High resolution T2-prepared MRI enables non-invasive assessment of CSF flow in perivascular spaces of the human brain. In: *ISMRM*; 2019:0746.
88. Wen Q, Tong Y, Zhou X, Dzemidzic M, Ho CY, Wu YC. Assessing pulsatile waveforms of paravascular cerebrospinal fluid dynamics within the glymphatic pathways using dynamic diffusion-weighted imaging (dDWI). *Neuroimage.* 2022;260:119464. doi:10.1016/j.neuroimage.2022.119464
89. Wen Q, Wright A, Tong Y, et al. Paravascular fluid dynamics reveal arterial stiffness assessed using dynamic diffusion-weighted imaging. *NMR Biomed.* 2024;37(2):e5048. doi:10.1002/nbm.5048
90. Sepehrband F, Cabeen RP, Barisano G, et al. Nonparenchymal fluid is the source of increased mean diffusivity in preclinical Alzheimer's disease. In: *Alzheimer's and Dementia: Diagnosis, Assessment and Disease Monitoring.* 2019;11(4):348-354. doi:10.1016/j.dadm.2019.03.002
91. Evans PG, Sajic M, Yu Y, et al. Changes in cardiac-driven perivascular fluid movement around the MCA in a pharmacological model of acute hypertension detected with non-invasive MRI. *J Cereb Blood Flow Metab.* 2023;44(4):508-515. doi:10.1177/0271678X231209641
92. Le Bihan D, Breton E, Lallemand D, et al. Contribution of Intravoxel Incoherent Motion (IVIM) imaging to neuroradiology. *J Neuroradiol.* 1987;14(4):295-312.
93. Steward CE, Venkatraman VK, Lui E, et al. Assessment of the DTI-ALPS parameter along the perivascular space in older adults at risk of dementia. *J Neuroimaging.* 2021;31(3):569-578. doi:10.1111/jon.12837
94. McKnight CD, Trujillo P, Lopez AM, et al. Diffusion along perivascular spaces reveals evidence supportive of glymphatic function impairment in Parkinson disease. *Parkinsonism Relat Disord.* 2021;89:98-104. doi:10.1016/j.parkreldis.2021.06.004
95. Chang HI, Huang CW, Hsu SW, et al. Gray matter reserve determines glymphatic system function in young-onset Alzheimer's disease: evidenced by DTI-ALPS and compared with age-matched controls. *Psychiatry Clin Neurosci.* 2023;77(7):401-409. doi:10.1111/pcn.13557

96. Qin Y, He R, Chen J, et al. Neuroimaging uncovers distinct relationships of glymphatic dysfunction and motor symptoms in Parkinson's disease. *J Neurol.* 2023;270(5):2649-2658. doi:10.1007/s00415-023-11594-5
97. Kamagata K, Andica C, Takabayashi K, et al. Association of MRI indices of glymphatic system with amyloid deposition and cognition in mild cognitive impairment and Alzheimer disease. *Neurology.* 2022;99(24):e2648-e2660. doi:10.1212/WNL.0000000000201300
98. Chen HL, Chen PC, Lu CH, et al. Associations among cognitive functions, plasma DNA, and diffusion tensor image along the perivascular space (DTI-ALPS) in patients with Parkinson's disease. *Oxid Med Cell Longev.* 2021;2021:4034509. doi:10.1155/2021/4034509
99. Hsu JL, Wei YC, Toh CH, et al. Magnetic resonance images implicate that glymphatic alterations mediate cognitive dysfunction in Alzheimer disease. *Ann Neurol.* 2023;93(1):164-174. doi:10.1002/ana.26516
100. Bae YJ, Kim JM, Choi BS, et al. Glymphatic function assessment in Parkinson's disease using diffusion tensor image analysis along the perivascular space. *Parkinsonism Relat Disord.* 2023;114:105767. doi:10.1016/j.parkreldis.2023.105767
101. Cai X, Chen Z, He C, et al. Diffusion along perivascular spaces provides evidence interlinking compromised glymphatic function with aging in Parkinson's disease. *CNS Neurosci Ther.* 2023;29(1):111-121. doi:10.1111/cns.13984
102. Gu L, Dai S, Guo T, et al. Noninvasive neuroimaging provides evidence for deterioration of the glymphatic system in Parkinson's disease relative to essential tremor. *Parkinsonism Relat Disord.* 2023;107:105254. doi:10.1016/j.parkreldis.2022.105254
103. Meng JC, Shen MQ, Lu YL, et al. Correlation of glymphatic system abnormalities with Parkinson's disease progression: a clinical study based on non-invasive fMRI. *J Neurol.* 2024;271(1):457-471. doi:10.1007/s00415-023-12004-6
104. Zhong J, Wang L, Li Y, Jiang J. A novel diffusion tensor image analysis along the perivascular space method to evaluate glymphatic alterations in Alzheimer's disease. In: *2023 45th Annual International Conference of the IEEE Engineering in Medicine & Biology Society (EMBC).* 2023:1-4. doi:10.1109/EMBC40787.2023.10340315
105. Saito Y, Kamagata K, Andica C, et al. Glymphatic system impairment in corticobasal syndrome: diffusion tensor image analysis along the perivascular space (DTI-ALPS). *Jpn J Radiol.* 2023;41(11):1226-1235. doi:10.1007/s11604-023-01454-7
106. Jiang D, Liu L, Kong Y, et al. Regional Glymphatic Abnormality in Behavioral Variant Frontotemporal Dementia. *Ann Neurol.* 2023;94(3):442-456. doi:10.1002/ana.26710
107. Zhang X, Wang Y, Jiao B, et al. Glymphatic system impairment in Alzheimer's disease: associations with perivascular space volume and cognitive function. *Eur Radiol.* 2024;34(2):1314-1323. doi:10.1007/s00330-023-10122-3
108. Tomizawa Y, Hagiwara A, Hoshino Y, et al. The glymphatic system as a potential biomarker and therapeutic target in secondary progressive multiple sclerosis. *Mult Scler Relat Disord.* 2024;83:105437. doi:10.1016/j.msard.2024.105437
109. Liang T, Chang F, Huang Z, Peng D, Zhou X, Liu W. Evaluation of glymphatic system activity by diffusion tensor image analysis along the perivascular space (DTI-ALPS) in dementia patients. *Br J Radiol.* 2023;96(1146):20220315. doi:10.1259/bjr.20220315
110. Yin Y, Peng Y, Nie L, et al. Impaired glymphatic system revealed by DTI-ALPS in cerebral palsy due to periventricular leukomalacia: relation with brain lesion burden and hand dysfunction. *Neuroradiology.* 2024;66(2):261-269. doi:10.1007/s00234-023-03269-9
111. Zhang W, Zhou Y, Wang J, et al. Glymphatic clearance function in patients with cerebral small vessel disease. *Neuroimage.* 2021;238:118257. doi:10.1016/j.neuroimage.2021.118257
112. Kikuta J, Kamagata K, Takabayashi K, et al. An investigation of water diffusivity changes along the perivascular space in elderly subjects with hypertension. *Am J Neuroradiol.* 2022;43(1):48-55. doi:10.3174/ajnr.A7334
113. Qin Y, Li X, Qiao Y, et al. DTI-ALPS: an MR biomarker for motor dysfunction in patients with subacute ischemic stroke. *Front Neurosci.* 2023;17:1132393. doi:10.3389/fnins.2023.1132393
114. Zhang C, Sha J, Cai L, et al. Evaluation of the glymphatic system using the DTI-ALPS index in patients with spontaneous intracerebral haemorrhage. *Oxid Med Cell Longev.* 2022;2022:1-7. doi:10.1155/2022/2694316
115. Tian Y, Cai X, Zhou Y, et al. Impaired glymphatic system as evidenced by low diffusivity along perivascular spaces is associated with cerebral small vessel disease: a population-based study. *Stroke Vasc Neurol.* 2023;8(5):e002191. doi:10.1136/svn-2022-002191
116. Wei YC, Hsu CCH, Huang WY, et al. Vascular risk factors and astrocytic marker for the glymphatic system activity. *Radiol Med.* 2023;128(9):1148-1161. doi:10.1007/s11547-023-01675-w
117. Wu CH, Kuo Y, Ling YH, et al. Dynamic changes in glymphatic function in reversible cerebral vasoconstriction syndrome. *J Headache Pain.* 2024;25(1):17. doi:10.1186/s10194-024-01726-1
118. Bae YJ, Choi BS, Kim JM, Choi JH, Cho SJ, Kim JH. Altered glymphatic system in idiopathic normal pressure hydrocephalus. *Parkinsonism Relat Disord.* 2021;82:56-60. doi:10.1016/j.parkreldis.2020.11.009
119. Kikuta J, Kamagata K, Taoka T, et al. Water diffusivity changes along the perivascular space after lumboperitoneal shunt surgery in idiopathic normal pressure hydrocephalus. *Front Neurol.* 2022;13:843883. doi:10.3389/fneur.2022.843883
120. Yokota H, Vijayasarathi A, Cekic M, et al. Diagnostic performance of glymphatic system evaluation using diffusion tensor imaging in idiopathic normal pressure hydrocephalus and mimickers. *Curr Gerontol Geriatr Res.* 2019;2019:5675014. doi:10.1155/2019/5675014
121. Georgiopoulos C, Tisell A, Holmgren RT, et al. Noninvasive assessment of glymphatic dysfunction in idiopathic normal pressure hydrocephalus with diffusion tensor imaging. *J Neurosurg.* 2023;140(3):612-620. doi:10.3171/2023.6.JNS23260
122. Lee DA, Lee J, Park KM. Glymphatic system impairment in patients with status epilepticus. *Neuroradiology.* 2022;64(12):2335-2342. doi:10.1007/s00234-022-03018-4
123. Zhang C, Xu K, Zhang H, et al. Recovery of glymphatic system function in patients with temporal lobe epilepsy after surgery. *Eur Radiol.* 2023;33(9):6116-6123. doi:10.1007/s00330-023-09588-y
124. Lee DA, Lee HJ, Park KM. Structural connectivity as a predictive factor for responsiveness to levetiracetam treatment in epilepsy. *Neuroradiology.* 2024;66(1):93-100. doi:10.1007/s00234-023-03261-3
125. Kim J, Lee DA, Lee H, Park KM. Glymphatic system dysfunction in patients with occipital lobe epilepsy. *J Neuroimaging.* 2023;33(3):455-461. doi:10.1111/jon.13083
126. Pu W, Wei S, Qiu M, et al. Dysfunction of the glymphatic system in childhood absence epilepsy. *Front Neurosci.* 2023;17:1312676. doi:10.3389/fnins.2023.1312676
127. Kim S, Kim SE, Lee DA, Lee H, Park KM. Anti-seizure medication response and the glymphatic system in patients with focal epilepsy. *Eur J Neurol.* 2024;31(1):e16097. doi:10.1111/ene.16097

128. Zhao X, Zhou Y, Li Y, et al. The asymmetry of glymphatic system dysfunction in patients with temporal lobe epilepsy: a DTI-ALPS study. *J Neuroradiol.* 2023;50(6):562-567. doi:10.1016/j.neurad.2023.05.009
129. Wu C, Chang F, Wang Y, et al. Impaired glymphatic and meningeal lymphatic functions in patients with chronic migraine. *Ann Neurol.* 2024;95(3): 583-595. doi:10.1002/ana.26842
130. Zhang X, Wang W, Bai X, et al. Increased glymphatic system activity in migraine chronification by diffusion tensor image analysis along the perivascular space. *J Headache Pain.* 2023;24(1):147. doi:10.1186/s10194-023-01673-3
131. Gumeler E, Aygun E, Tezer FI, Saritas EU, Oguz KK. Assessment of glymphatic function in narcolepsy using DTI-ALPS index. *Sleep Med.* 2023;101: 522-527. doi:10.1016/j.sleep.2022.12.002
132. Bae YJ, Kim JM, Choi BS, et al. Altered brain glymphatic flow at diffusion-tensor MRI in rapid eye movement sleep behavior disorder. *Radiology*. 2023;307(5):e221848. doi:10.1148/radiol.221848
133. Saito Y, Hayakawa Y, Kamagata K, et al. Glymphatic system impairment in sleep disruption: diffusion tensor image analysis along the perivascular space (DTI-ALPS). *Jpn J Radiol.* 2023;41(12):1335-1343. doi:10.1007/s11604-023-01463-6
134. Yang D, Sun Z, Yu M, et al. Associations of MRI-derived glymphatic system impairment with global white matter damage and cognitive impairment in mild traumatic brain injury: a DTI-ALPS study. *J Magn Reson Imaging.* 2024;59(2):639-647. doi:10.1002/jmri.28797
135. Butler T, Zhou L, Ozsahin I, et al. Glymphatic clearance estimated using diffusion tensor imaging along perivascular spaces is reduced after traumatic brain injury and correlates with plasma neurofilament light, a biomarker of injury severity. *Brain Commun.* 2023;5(3):fcad134. doi:10.1093/braincomms/fcad134
136. Morita Y, Kamagata K, Andica C, et al. Glymphatic system impairment in nonathlete older male adults who played contact sports in their youth associated with cognitive decline: A diffusion tensor image analysis along the perivascular space study. *Front Neurol.* 2023;14:1100736. doi:10.3389/fneur.2023.1100736
137. Park JH, Bae YJ, Kim JS, et al. Glymphatic system evaluation using diffusion tensor imaging in patients with traumatic brain injury. *Neuroradiology*. 2023;65(3):551-557. doi:10.1007/s00234-022-03073-x
138. Taoka T, Ito R, Nakamichi R, et al. Diffusion-weighted image analysis along the perivascular space (DWI–ALPS) for evaluating interstitial fluid status: age dependence in normal subjects. *Jpn J Radiol.* 2022;40(9):894-902. doi:10.1007/s11604-022-01275-0
139. Drenthen GS, Elschot EP, van der Knaap N, et al. Imaging interstitial fluid with MRI: a narrative review on the associations of altered interstitial fluid with vascular and neurodegenerative abnormalities. *J Magn Reson Imaging.* 2023; Epub ahead of print. doi:10.1002/jmri.29056
140. Park CJ, Kim SY, Kim JH, et al. Evaluation of glymphatic system activity using diffusion tensor image analysis along the perivascular space and amyloid PET in older adults with objectively normal cognition: a preliminary study. *Front Aging Neurosci.* 2023;15:1221667. doi:10.3389/fnagi.2023.1221667
141. Wang J, Zhou Y, Zhang K, et al. Glymphatic function plays a protective role in ageing-related cognitive decline. *Age Ageing.* 2023;52(7):afad107. doi:10.1093/ageing/afad107
142. Hsiao WC, Chang HI, Hsu SW, et al. Association of cognition and brain reserve in aging and glymphatic function using diffusion tensor image-along the perivascular space (DTI-ALPS). *Neuroscience.* 2023;524:11-20. doi:10.1016/j.neuroscience.2023.04.004
143. Ringstad G. Glymphatic imaging: a critical look at the DTI-ALPS index. *Neuroradiology.* 2024;66(2):157-160. doi:10.1007/s00234-023-03270-2
144. Wright AM, Wu Y, Chen N, Wen Q. Exploring radial asymmetry in MR diffusion tensor imaging and its impact on the interpretation of glymphatic mechanisms. *J Magn Reson Imaging.* 2023; Epub ahead of print. doi:10.1002/jmri.29203
145. Taoka T, Ito R, Nakamichi R, et al. Reproducibility of diffusion tensor image analysis along the perivascular space (DTI-ALPS) for evaluating interstitial fluid diffusivity and glymphatic function: CHanges in Alps index on Multiple conditiON acquIsition eXperiment (CHAMONIX) study. *Jpn J Radiol*. 2022;40(2):147-158. doi:10.1007/s11604-021-01187-5
146. Alexander AL, Hasan KM, Lazar M, Tsuruda JS, Parker DL. Analysis of partial volume effects in diffusion-tensor MRI. *Magn Reson Med.* 2001;45(5): 770-780. doi:10.1002/mrm.1105
147. Pierpaoli C, Jones DK. Removing CSF contamination in brain DT-MRIs by using a two-compartment tensor model. In: *Proceedings of the 12th Annual Meeting of ISMRM, Kyoto*; 2004.
148. Lynch KM, Sepehrband F, Toga AW, Choupan J. Brain perivascular space imaging across the human lifespan. *Neuroimage.* 2023;271:120009. doi:10.1016/j.neuroimage.2023.120009
149. Le Bihan D, Breton E, Lallemand D, Grenier P, Cabanis E, Laval-Jeantet M. MR imaging of intravoxel incoherent motions: application to diffusion and perfusion in neurologic disorders. *Radiology*. 1986;161(2):401-407. doi:10.1148/radiology.161.2.3763909
150. Le Bihan D, Breton E, Lallemand D, Aubin ML, Vignaud J, Laval-Jeantet M. Separation of diffusion and perfusion in intravoxel incoherent motion MR imaging. *Radiology*. 1988;168(2):497-505. doi:10.1148/radiology.168.2.3393671
151. Le Bihan D. What can we see with IVIM MRI? *Neuroimage.* 2019;187:56-67. doi:10.1016/j.neuroimage.2017.12.062
152. Federau C, Hagmann P, Maeder P, et al. Dependence of brain intravoxel incoherent motion perfusion parameters on the cardiac cycle. *PLoS ONE*. 2013;8(8):e72856. doi:10.1371/journal.pone.0072856
153. Yamada S, Ishikawa M, Yamamoto K. Fluid distribution pattern in adult-onset congenital, idiopathic, and secondary normal-pressure hydrocephalus: Implications for clinical care. *Front Neurol.* 2017;8:583. doi:10.3389/fneur.2017.00583
154. Yamada S, Ishikawa M, Yamamot K. Optimal diagnostic indices for idiopathic normal pressure hydrocephalus based on the 3D quantitative volumetric analysis for the cerebral ventricle and subarachnoid space. *Am J Neuroradiol.* 2015;36(12):2262-2269. doi:10.3174/ajnr.A4440
155. Yamada S, Ishikawa M, Yamamoto K. Comparison of CSF distribution between idiopathic normal pressure hydrocephalus and Alzheimer disease. *Am J Neuroradiol.* 2016;37(7):1249-1255. doi:10.3174/ajnr.A4695
156. Yamada S, Ishikawa M, Yamaguchi M, Yamamoto K. Longitudinal morphological changes during recovery from brain deformation due to idiopathic normal pressure hydrocephalus after ventriculoperitoneal shunt surgery. *Sci Rep.* 2019;9(1):17318. doi:10.1038/s41598-019-53888-7
157. Wu W, Wong E. The effects of water diffusion and laminar flow on velocity-selective arterial spin labeling. In: *Annual International Conference of the IEEE Engineering in Medicine and Biology - Proceedings*. Vol.26 III; 2004. doi:10.1109/iembs.2004.1403559
158. Wu WC, Chen YF, Tseng HM, Yang SC, My PC. Caveat of measuring perfusion indexes using intravoxel incoherent motion magnetic resonance imaging in the human brain. *Eur Radiol.* 2015;25(8):2485-2492. doi:10.1007/s00330-015-3655-x

159. Barbieri S, Donati OF, Froehlich JM, Thoeny HC. Comparison of intravoxel incoherent motion parameters across MR imagers and field strengths: Evaluation in upper abdominal organs. *Radiology*. 2016;279(3):784-794. doi:10.1148/radiol.2015151244
160. Cohen AD, Schieke MC, Hohenwalter MD, Schmainda KM. The effect of low b-values on the intravoxel incoherent motion derived pseudodiffusion parameter in liver. *Magn Reson Med*. 2015;73(1):306-311. doi:10.1002/mrm.25109
161. Meeus EM, Novak J, Withey SB, Zarinabad N, Dehghani H, Peet AC. Evaluation of intravoxel incoherent motion fitting methods in low-perfused tissue. *J Magn Reson Imaging*. 2017;45(5):1325-1334. doi:10.1002/jmri.25411
162. Olesen JL, Østergaard L, Shemesh N, Jespersen SN. Diffusion time dependence, power-law scaling, and exchange in gray matter. *Neuroimage*. 2022;251:118976. doi:10.1016/j.neuroimage.2022.118976
163. Jelescu IO, de Skowronski A, Geffroy F, Palombo M, Novikov DS. Neurite Exchange Imaging (NEXI): a minimal model of diffusion in gray matter with inter-compartment water exchange. *Neuroimage*. 2022;256:119277. doi:10.1016/j.neuroimage.2022.119277
164. Zhang H, Schneider T, Wheeler-Kingshott CA, Alexander DC. NODDI: practical in vivo neurite orientation dispersion and density imaging of the human brain. *Neuroimage*. 2012;61(4):1000-1016. doi:10.1016/j.neuroimage.2012.03.072
165. Wen Q, Kelley DAC, Banerjee S, et al. Clinically feasible NODDI characterization of glioma using multiband EPI at 7 T. *Neuroimage Clin*. 2015;9:291-299. doi:10.1016/j.nicl.2015.08.017
166. Wen Q, Mustafi SM, Li J, et al. White matter alterations in early-stage Alzheimer's disease: a tract-specific study. In: *Alzheimer's and Dementia: Diagnosis, Assessment and Disease Monitoring*. Vol.11; 2019. doi:10.1016/j.dadm.2019.06.003
167. Kamiya K, Hori M, Aoki S. NODDI in clinical research. *J Neurosci Methods*. 2020;346:108908. doi:10.1016/j.jneumeth.2020.108908
168. Colgan N, Siow B, O'Callaghan JM, et al. Application of neurite orientation dispersion and density imaging (NODDI) to a tau pathology model of Alzheimer's disease. *Neuroimage*. 2016;125:739-744. doi:10.1016/j.neuroimage.2015.10.043
169. Williamson NH, Komlosh ME, Benjamini D, Basser PJ. Limits to flow detection in phase contrast MRI. *J Magn Reson Open*. 2020;2-3:100004. doi:10.1016/j.jmro.2020.100004
170. Wong EC, Cox RW, Song AW. Optimized isotropic diffusion weighting. *Magn Reson Med*. 1995;34(2):139-143. doi:10.1002/mrm.1910340202

How to cite this article: Wright AM, Wu Y-C, Feng L, Wen Q. Diffusion magnetic resonance imaging of cerebrospinal fluid dynamics: Current techniques and future advancements. *NMR in Biomedicine*. 2024;e5162. doi:10.1002/nbm.5162